

# Coupling of Particle Filters<sup>\*</sup>

Pierre E. Jacob<sup>†</sup>

Department of Statistics, Harvard University

Fredrik Lindsten and Thomas B. Schön

Department of Information Technology, Uppsala University

July 19, 2016

## Abstract

Particle filters provide Monte Carlo approximations of intractable quantities such as point-wise evaluations of the likelihood in state space models. In many scenarios, the interest lies in the comparison of these quantities as some parameter or input varies. To facilitate such comparisons, we introduce and study methods to couple two particle filters in such a way that the correlation between the two underlying particle systems is increased. The motivation stems from the classic variance reduction technique of positively correlating two estimators. The key challenge in constructing such a coupling stems from the discontinuity of the resampling step of the particle filter. As our first contribution, we consider coupled resampling algorithms. Within bootstrap particle filters, they improve the precision of finite-difference estimators of the score vector and boost the performance of particle marginal Metropolis–Hastings algorithms for parameter inference. The second contribution arises from the use of these coupled resampling schemes within conditional particle filters, allowing for unbiased estimators of smoothing functionals. The result is a new smoothing strategy that operates by averaging a number of independent and unbiased estimators, which allows for 1) straightforward parallelization and 2) the construction of accurate error estimates. Neither of the above is possible with existing particle smoothers.

*Keywords:* common random numbers, couplings, optimal transport, particle filtering, particle smoothing, resampling algorithms

## 1 Introduction

In the context of nonlinear state space models, particle filters provide efficient approximations of the distribution of a latent process  $(x_t)_{t \geq 0}$ , given noisy and partial observations  $(y_t)_{t \geq 1}$  (Doucet

---

<sup>\*</sup>This research is financially supported by the Swedish Foundation for Strategic Research (SSF) via the project *ASSEMBLE* and the Swedish research Council (VR) via the projects *Learning of complex dynamical systems* (Contract number: 637-2014-466) and *Probabilistic modeling of dynamical systems* (Contract number: 621-2013-5524).

<sup>†</sup>Corresponding author: pjacob@fas.harvard.edu. Code available at: [github.com/pierrejacob/](https://github.com/pierrejacob/).

et al., 2001; Cappé et al., 2005; Doucet and Johansen, 2011). We assume that the latent process takes values in  $\mathbb{X} \subset \mathbb{R}^{d_x}$ , and that the observations are in  $\mathbb{Y} \subset \mathbb{R}^{d_y}$  for some  $d_x, d_y \in \mathbb{N}$ . The model specifies an initial distribution  $m_0(dx_0|\theta)$  and a transition kernel  $f(dx_t|x_{t-1}, \theta)$  for the Markovian latent process. Conditionally upon the latent process, the observations are independent and their distribution is given by a measurement kernel  $g(dy_t|x_t, \theta)$ . The model is parameterized by  $\theta \in \Theta \subset \mathbb{R}^{d_\theta}$ , for  $d_\theta \in \mathbb{N}$ . Filtering consists in approximating the distribution  $p(dx_t|y_{1:t}, \theta)$  for all times  $t \geq 1$ , whereas smoothing consists in approximating the distribution  $p(dx_{0:T}|y_{1:T}, \theta)$  for a fixed time horizon  $T$ , where for  $s, t \in \mathbb{N}$ , we write  $s:t$  for the set  $\{s, \dots, t\}$ , and  $v_{s:t}$  for the vector  $(v_s, \dots, v_t)$ .

The bootstrap particle filter (Gordon et al., 1993) generates weighted samples denoted by  $(w_t^k, x_t^k)_{k=1}^N$ , for all  $t \in \mathbb{N}$ , where the particle locations  $(x_t^k)_{k=1}^N$  are samples in  $\mathbb{X}$  and the weights  $(w_t^k)_{k=1}^N$  are non-negative reals summing to one. The number  $N \in \mathbb{N}$  of particles is specified by the user—the computational cost of the algorithm is linear in  $N$ , while the approximation of  $p(dx_t|y_{1:t}, \theta)$  by  $\sum_{k=1}^N w_t^k \delta_{x_t^k}(dx_t)$  becomes more precise as  $N$  increases (e.g. Del Moral, 2004; Whiteley, 2013, and references therein). An important by-product of the particle filter for statistical inference is the likelihood estimator, defined as  $\hat{p}^N(y_{1:t}|\theta) := \prod_{s=1}^t N^{-1} \sum_{k=1}^N g(y_s|x_s^k, \theta)$ . The likelihood estimator is known to have expectation equal to the likelihood  $p(y_{1:t}|\theta)$ , and its variance has been extensively studied (Del Moral, 2004; Cérou et al., 2011; Bérard et al., 2014). The estimator is at the core of the particle marginal Metropolis–Hastings (MH) algorithm (Andrieu et al., 2010; Doucet et al., 2015), in which particle filters are run within an MH scheme, enabling inference in a large class of state space models.

We consider methods to couple particle filters. A coupling of particle filters, given two parameter values  $\theta$  and  $\tilde{\theta}$ , refers to a pair of particle systems, denoted by  $(w_t^k, x_t^k)_{k=1}^N$  and  $(\tilde{w}_t^k, \tilde{x}_t^k)_{k=1}^N$ , such that: 1) marginally, each system has the same distribution as if it was generated by a particle filter, respectively given  $\theta$  and  $\tilde{\theta}$ , and 2) the two systems are in some sense correlated. The same couplings can be applied to pairs of conditional particle filters (Andrieu et al., 2010), which are conditioned on different reference trajectories, instead of different parameters. In the case of particle filters, the goal is to introduce positive correlations between likelihood estimators  $\hat{p}^N(y_{1:t}|\theta)$  and  $\hat{p}^N(y_{1:t}|\tilde{\theta})$ , which improves the performance of score estimators and of MH schemes (Deligiannidis et al., 2015; Dahlin et al., 2015). In the case of conditional particle filters, couplings lead to a new algorithm for smoothing, which is trivial to parallelize, provides unbiased estimators of smoothing functionals and accurate estimates of the associated Monte Carlo error.

Correlating estimators is a classic Monte Carlo technique for variance reduction, and can often be achieved by using common random numbers (Kahn and Marshall, 1953; Asmussen and Glynn, 2007; Glasserman and Yao, 1992). Particle filters are randomized algorithms which can be written as a deterministic function of some random variables and a parameter value. However, they are discontinuous functions of their inputs, due to the resampling steps. This discontinuity renders theoretical guarantees supporting the use of common random numbers such as Proposition 2.2 in Glasserman and Yao (1992) inapplicable. Despite various attempts (see Pitt, 2002; Lee, 2008; Malik

and Pitt, 2011, and references therein), there are no standard ways of coupling particle filters. Our proposed strategy relies on common random numbers for the initialization and propagation steps, while the resampling step is performed jointly for a pair of particle systems, using ideas inspired by maximal couplings and optimal transport ideas.

Coupled resampling schemes and coupled particle filters are described in Section 2. In Section 3, they are shown to lead to various methodological developments: in particular, they are instrumental in the construction of a new smoothing estimator, in combination with the debiasing technique of Glynn and Rhee (2014). In Section 4, numerical results illustrate the gains brought by coupled particle filters in a real-world prey-predator model, and Section 5 concludes. The appendices contain various additional descriptions, proofs and extra numerical results.

## 2 Coupled resampling

### 2.1 Common random numbers

Within particle filters, random variables are used to initialize, to resample and to propagate the particles. We describe bootstrap particle filters in that light. Initially, we sample  $x_0^k \sim m_0(dx_0|\theta)$  for all  $k \in 1 : N$ , or equivalently, we compute  $x_0^k = M(U_0^k, \theta)$  where  $M$  is a function and  $U_0^{1:N}$  random variables. The initial weights  $w_0^k$  are set to  $N^{-1}$ . Consider now step  $t \geq 0$  of the algorithm. In the resampling step, a vector of ancestor variables  $a_t^{1:N} \in \{1, \dots, N\}^N$  is sampled. The resampling step can be written  $a_t^{1:N} \sim r(da^{1:N}|w_t^{1:N})$ , for some distribution  $r$ . The propagation step consists in drawing  $x_{t+1}^k \sim f(dx_{t+1}|x_t^{a_t^k}, \theta)$ , or equivalently, computing  $x_{t+1}^k = F(x_t^{a_t^k}, U_{t+1}^k, \theta)$ , where  $F$  is a function and  $U_{t+1}^{1:N}$  random variables. The next weights are computed as  $w_{t+1}^k \propto g(y_{t+1}|x_{t+1}^k, \theta)$ , then normalized to sum to one; and the algorithm proceeds. We refer to  $U_t^{1:N}$  for all  $t$  as the process-generating variables. The resampling distribution  $r$  is an algorithmic choice; a standard condition for its validity is that, under  $r$ ,  $\mathbb{P}(a_t^k = j) = w_t^j$ ; various schemes satisfying this condition exist (e.g. Douc and Cappé, 2005; Murray et al., 2015).

Consider a pair of particle filters given  $\theta$  and  $\tilde{\theta}$ , producing particle systems  $(w_t^k, x_t^k)_{k=1}^N$  and  $(\tilde{w}_t^k, \tilde{x}_t^k)_{k=1}^N$ , that we want to make as correlated as possible. Assume that the state space is one-dimensional, that  $u \mapsto M(u, \theta)$  and  $u \mapsto M(u, \tilde{\theta})$  are increasing and right-continuous, and that  $\mathbb{E}[M^2(U_0, \theta)] < \infty$  and  $\mathbb{E}[M^2(U_0, \tilde{\theta})] < \infty$ . Then Proposition 2.2 of Glasserman and Yao (1992) states that the correlation between  $M(U_0, \theta)$  and  $M(V_0, \tilde{\theta})$  is maximized, among all choices of joint distributions for  $(U_0, V_0)$  that have the same marginal distributions, by choosing  $U_0 = V_0$  almost surely. This justifies the use of common random numbers for the initialization step. Likewise, if the propagation function  $F : (x_t, U_{t+1}, \theta) \mapsto x_{t+1}$  is continuous in its first and third arguments, and if the particle locations  $x_t$  and  $\tilde{x}_t$  are similar, then, intuitively,  $x_{t+1} = F(x_t, U_{t+1}, \theta)$  and  $\tilde{x}_{t+1} = F(\tilde{x}_t, U_{t+1}, \tilde{\theta})$  should be similar as well. The difficulty comes from the resampling step. We can write  $a_t^{1:N} = R(w_t^{1:N}, U_{R,t})$ , where  $U_{R,t}$  are random variables, typically uniformly distributed.

Since the resampling function  $(w_t^{1:N}, U_{R,t}) \mapsto a_t^{1:N} = R(w_t^{1:N}, U_{R,t})$  takes values in the discrete space  $\{1, \dots, N\}^N$ , it cannot be a continuous function of its arguments. In other words, even if we use the same random numbers for  $U_{R,t}$ , a small difference between the weight vectors  $w_t^{1:N}$  and  $\tilde{w}_t^{1:N}$  might lead to sampling, for instance,  $a_t^k = i$  in the first system and  $\tilde{a}_t^k = i + 1$  in the second system; and  $x_t^i$  and  $\tilde{x}_t^{i+1}$  have no reason to be similar. This leads to discontinuities in by-products of the particle system, such as the likelihood estimator  $\hat{p}^N(y_{1:T}|\theta)$  as a function of  $\theta$ , for fixed common random numbers. We thus separate the randomness in process-generating variables from the resampling step, and consider resampling algorithms designed to correlate the particles in both systems.

## 2.2 Coupled resampling and coupled particle filters

We use bold fonts to denote vectors of objects indexed by  $k \in 1 : N$ , for instance  $(\mathbf{w}_t, \mathbf{x}_t) = (w_t^k, x_t^k)_{k=1}^N$  or  $\mathbf{U}_t = U_t^{1:N}$ , and we drop the temporal notation whenever possible, for clarity. We consider the problem of jointly resampling  $(\mathbf{w}, \mathbf{x})$  and  $(\tilde{\mathbf{w}}, \tilde{\mathbf{x}})$ . A joint distribution on  $\{1, \dots, N\}^2$  is characterized by a matrix  $P$  with non-negative entries  $P^{ij}$ , for  $i, j \in \{1, \dots, N\}$ , that sum to one. The value  $P^{ij}$  represents the probability of sampling the pair  $(i, j)$ . We consider the set  $\mathcal{J}(\mathbf{w}, \tilde{\mathbf{w}})$  of matrices  $P$  such that  $P\mathbf{1} = \mathbf{w}$  and  $P^\top \mathbf{1} = \tilde{\mathbf{w}}$ , where  $\mathbf{1}$  denotes a column vector of  $N$  ones. Pairs  $(\mathbf{a}, \tilde{\mathbf{a}})$  distributed according to  $P \in \mathcal{J}(\mathbf{w}, \tilde{\mathbf{w}})$  are such that  $\mathbb{P}(a^k = j) = w^j$  and  $\mathbb{P}(\tilde{a}^k = j) = \tilde{w}^j$  for all  $k$  and  $j$ . The choice  $P = \mathbf{w} \tilde{\mathbf{w}}^\top$  corresponds to an independent coupling of  $\mathbf{w}$  and  $\tilde{\mathbf{w}}$ . Sampling from this matrix  $P$  is done by sampling  $\mathbf{a}$  with probabilities  $\mathbf{w}$  and  $\tilde{\mathbf{a}}$  with probabilities  $\tilde{\mathbf{w}}$ , independently.

Any choice of probability matrix  $P \in \mathcal{J}(\mathbf{w}, \tilde{\mathbf{w}})$  leads to a coupled resampling scheme, and to a coupled bootstrap particle filter that proceeds as follows. The initialization and propagation steps are performed as in the standard particle filter, using common process-generating variables  $\mathbf{U}_{0:T}$  and the parameter values  $\theta$  and  $\tilde{\theta}$  respectively. At each step  $t \geq 0$ , the resampling step involves computing a matrix  $P_t$  in  $\mathcal{J}(\mathbf{w}, \tilde{\mathbf{w}})$ , possibly using all the variables generated thus far. Then the pairs of ancestors  $(\mathbf{a}_t, \tilde{\mathbf{a}}_t)$  are sampled from  $P_t$ .

Coupled resampling schemes can be applied in generic particle methods beyond the bootstrap filter. We illustrate this generality by coupling conditional particle filters. Given a trajectory  $X = x_{0:T}$ , referred to as the reference trajectory, and process-generating variables  $\mathbf{U}_{0:T}$ , the conditional particle filter defines a distribution on the space of trajectories, as follows. At the initial step, we compute  $x_0^k = M(U_0^k, \theta)$  for all  $k \in 1 : N - 1$ , we set  $x_0^N = x_0$ , and  $w_0^k = N^{-1}$  for all  $k$ . At each step  $t$ , we draw  $a_t^{1:N-1} \sim r(da^{1:N-1} | w_t^{1:N})$  from a multinomial distribution, and set  $a_t^N = N$ ; other resampling schemes can be implemented, as detailed in [Chopin and Singh \(2015\)](#). The propagation step computes  $x_{t+1}^k = F(x_t^{a_t^k}, U_{t+1}^k, \theta)$  for  $k \in 1 : N - 1$  and sets  $x_{t+1}^N = x_{t+1}$ . The weighting step computes  $w_{t+1}^k \propto g(y_{t+1} | x_{t+1}^k, \theta)$ , for all  $k \in 1 : N$ . The procedure guarantees that the reference trajectory  $x_{0:T}$  is among the trajectories produced by the algorithm. At the final step, we draw

$b_T$  with probabilities  $\mathbf{w}_T$  and retrieve the corresponding trajectory, denoted  $X'$ . The coupled conditional particle filter acts similarly, producing a pair of trajectories  $(X', \tilde{X}')$  given a pair of reference trajectories  $X = x_{0:T}$  and  $\tilde{X} = \tilde{x}_{0:T}$ . The initialization and propagation steps follow the conditional particle filter for each system, using common random numbers  $\mathbf{U}_{0:T}$ . For the resampling step, we compute a probability matrix  $P_t \in \mathcal{J}(\mathbf{w}_t, \tilde{\mathbf{w}}_t)$ , based on the variables generated thus far, and we sample pairs of ancestor variables  $(a_t^k, \tilde{a}_t^k)_{k=1}^{N-1}$ . We then set  $a_t^N = N$  and  $\tilde{a}_t^N = N$ . At the final step, we draw a pair of indices  $(b_T, \tilde{b}_T)$  from  $P_T$ , a probability matrix in  $\mathcal{J}(\mathbf{w}_T, \tilde{\mathbf{w}}_T)$ , and retrieve the corresponding pair of trajectories. The coupled conditional particle filter leads to a new smoothing algorithm, described in Section 3.3.

We now investigate particular choices of matrices  $P \in \mathcal{J}(\mathbf{w}_t, \tilde{\mathbf{w}}_t)$  with the aim of correlating a pair of particle systems.

### 2.3 Transport resampling

Intuitively, we want to choose  $P \in \mathcal{J}(\mathbf{w}, \tilde{\mathbf{w}})$  such that, upon sampling ancestors from  $P$ , the resampled particles are as similar as possible between the two systems. Similarity between locations can be encoded by a distance  $d : \mathbb{X} \times \mathbb{X} \rightarrow \mathbb{R}^+$ , for instance the Euclidean distance in  $\mathbb{X} \subset \mathbb{R}^{d_x}$ . The expected distance between the resampled particles  $\mathbf{x}^a$  and  $\tilde{\mathbf{x}}^{\tilde{a}}$ , conditional upon  $(\mathbf{w}, \mathbf{x})$  and  $(\tilde{\mathbf{w}}, \tilde{\mathbf{x}})$ , is given by  $\sum_{i=1}^N \sum_{j=1}^N P^{ij} d(x^i, \tilde{x}^j)$ . Denote by  $D$  the distance matrix with entries  $D^{ij} = d(x^i, \tilde{x}^j)$ . The optimal transport problem considers a matrix  $P^*$  that minimizes the expected distance over all  $P \in \mathcal{J}(\mathbf{w}, \tilde{\mathbf{w}})$ . Computing  $P^*$ , either exactly or approximately, is the topic of a rich literature. Exact algorithms compute  $P^*$  in order  $N^3 \log N$  operations, while recent methods introduce regularized solutions  $P^\varepsilon$ , where  $\varepsilon \in (0, \infty)$  is such that  $P^\varepsilon \rightarrow P^*$  when  $\varepsilon \rightarrow 0$ . The regularized solution  $P^\varepsilon$  is then approximated by an iterative algorithm, yielding a matrix  $\hat{P}$  in order  $N^2$  operations (Cuturi, 2013; Benamou et al., 2015). Computing the distance matrix  $D$  and sampling from a generic probability matrix  $P$  already cost  $N^2$  operations in general, thus the overall cost is in  $N^2$  operations. We denote by  $\hat{P}$  the matrix obtained by Cuturi's approximation (Cuturi, 2013).

Unlike the exact solution  $P^*$  and its regularized approximation  $P^\varepsilon$ , an approximate solution  $\hat{P}$  might not belong to  $\mathcal{J}(\mathbf{w}, \tilde{\mathbf{w}})$ . Directly using such a  $\hat{P}$  in a coupled particle filter would result in a bias, for instance in the likelihood estimator. However, we can easily construct a matrix  $P \in \mathcal{J}(\mathbf{w}, \tilde{\mathbf{w}})$  that is close to  $\hat{P}$ . Introduce  $\mathbf{u} = \hat{P}\mathbf{1}$  and  $\tilde{\mathbf{u}} = \hat{P}^\top \mathbf{1}$ , the marginals of  $\hat{P}$ . We compute a new matrix  $P$  as  $P = \alpha \hat{P} + (1 - \alpha) \mathbf{r} \tilde{\mathbf{r}}^\top$  for some  $\alpha \in [0, 1]$  and some probability vectors  $\mathbf{r}$  and  $\tilde{\mathbf{r}}$ . The marginal constraints yield a system to solve for  $\mathbf{r}$ ,  $\tilde{\mathbf{r}}$  and  $\alpha$ . We obtain  $\mathbf{r} = (\mathbf{w} - \alpha \mathbf{u}) / (1 - \alpha)$ ,  $\tilde{\mathbf{r}} = (\tilde{\mathbf{w}} - \alpha \tilde{\mathbf{u}}) / (1 - \alpha)$ , and  $0 \leq \alpha \leq \min_{i \in 1:N} \min(w^i / u^i, \tilde{w}^i / \tilde{u}^i)$ . To make the best use of the transport matrix  $\hat{P}$ , we select  $\alpha$  to attain the upper bound. Following Cuturi (2013), we choose  $\varepsilon$  as a small proportion of the median of the distance matrix  $D$ . As a stopping criterion for the iterative algorithm yielding  $\hat{P}$ , we can select  $\alpha$  as a desired value close to one, and run the iterative

algorithm until the value can be chosen, i.e. until  $\alpha \leq \min_{i \in 1:N} \min(w^i/u^i, \tilde{w}^i/\tilde{u}^i)$ .

The computational cost of transport resampling is potentially prohibitive, but it is model-independent and linear in the dimension  $d_x$  of the state space. Furthermore the active research area of numerical transport might provide faster algorithms in the future. Thus, for complex dynamical systems, the cost of transport resampling might still be negligible compared to the cost of the propagation steps.

## 2.4 Index-coupled resampling

Next we consider a computationally cheaper alternative to transport resampling termed *index-coupled* resampling. This scheme was used by [Chopin and Singh \(2015\)](#) in their theoretical analysis of the conditional particle filter. It has also been used by [Jasra et al. \(2015\)](#) in the setting of multilevel Monte Carlo. Its computational cost is linear in  $N$ . The idea of index-coupling is to maximize the probability of sampling pairs  $(a, \tilde{a})$  such that  $a = \tilde{a}$ , by computing the matrix  $P \in \mathcal{J}(\mathbf{w}, \tilde{\mathbf{w}})$  with maximum entries on its diagonal. The scheme is intuitive at the initial step of the algorithm, assuming that  $\theta$  and  $\tilde{\theta}$  are similar. At step  $t$ , the same random number  $U_t^k$  is used to compute  $x_t^k$  and  $\tilde{x}_t^k$  from their ancestors. Therefore, by sampling  $a_t^k = \tilde{a}_t^k$ , we select pairs that were computed with common random numbers at the previous step, and give them common random numbers  $U_{t+1}^k$  again. The scheme maximizes the number of consecutive steps where common random numbers are given to each pair. We describe how to implement the scheme, in the spirit of maximal couplings ([Lindvall, 2002](#)), before providing more intuition.

First, for all  $i \in 1 : N$ ,  $P$  has to satisfy  $P^{ii} \leq \min(w^i, \tilde{w}^i)$ , otherwise one of the marginal constraints would be violated. We tentatively write  $P = \alpha \text{diag}(\boldsymbol{\mu}) + (1 - \alpha)R$ , where  $\boldsymbol{\nu} = \min(\mathbf{w}, \tilde{\mathbf{w}})$  (element-wise),  $\alpha = \sum_{i=1}^N \nu^i$ ,  $\boldsymbol{\mu} = \boldsymbol{\nu}/\alpha$  and  $R$  is a residual matrix with zeros on the diagonal. Matrices  $P$  of this form have maximum trace among all matrices in  $\mathcal{J}(\mathbf{w}, \tilde{\mathbf{w}})$ . We now look for  $R$  such that  $P \in \mathcal{J}(\mathbf{w}, \tilde{\mathbf{w}})$  and such that sampling from  $P$  can be done linearly in  $N$ . From the marginal constraints, the matrix  $R$  needs to satisfy, for all  $i \in 1 : N$ ,  $\nu^i + (1 - \alpha) \sum_{j=1}^N R^{ij} = w^i$  and  $\nu^i + (1 - \alpha) \sum_{j=1}^N R^{ji} = \tilde{w}^i$ . Among all the matrices  $R$  that satisfy these constraints, the choice  $R = \mathbf{r}\tilde{\mathbf{r}}^\top$ , where  $\mathbf{r} = (\mathbf{w} - \boldsymbol{\nu})/(1 - \alpha)$  and  $\tilde{\mathbf{r}} = (\tilde{\mathbf{w}} - \boldsymbol{\nu})/(1 - \alpha)$ , is such that we can sample pairs of indices from  $R$  by sampling from  $\mathbf{r}$  and  $\tilde{\mathbf{r}}$  independently, for a linear cost in  $N$ . Thus we define the index-coupled matrix  $P$  as

$$P = \alpha \text{diag}(\boldsymbol{\mu}) + (1 - \alpha) \mathbf{r}\tilde{\mathbf{r}}^\top. \quad (1)$$

Under model assumptions, using common random numbers to propagate a pair of particles will result in the pair of states getting closer. We can formulate assumptions on the function  $(x, \theta) \mapsto \mathbb{E}[F(x, U, \theta)]$  as a function of both of its arguments, where the expectation is with respect to  $U$ . We can assume for instance that it is Lipschitz in both arguments. In an auto-regressive model where  $F(x, U, \theta) = \theta X + U$ , the Lipschitz constant is  $x$  as a function of  $\theta$  and  $\theta$  as a function

of  $x$ . One can then find conditions (see e.g. [Diaconis and Freedman, 1999](#)) such that the distance between the two propagated particles will decrease down to a value proportional to the distance between  $\theta$  and  $\tilde{\theta}$ , when common random numbers are used to propagate the pair.

We will see in [Section 4](#) that index-coupled resampling can perform essentially as well as transport resampling in real-world models.

## 2.5 Existing approaches

Various attempts have been made to modify particle filters so that they produce correlated likelihood estimators. A detailed review is given in [Lee \(2008\)](#). We describe the method proposed in [Pitt \(2002\)](#), which is based on sorting the particles. Consider first the univariate case,  $d_x = 1$ . We can sort both particle systems in increasing order of  $x^{1:N}$  and  $\tilde{x}^{1:N}$  respectively, yielding  $(w^{(k)}, x^{(k)})$  and  $(\tilde{w}^{(k)}, \tilde{x}^{(k)})$  for  $k \in 1 : N$ , where the parenthesis indicate that the samples are sorted. Then, we can draw  $a^{1:N}$  and  $\tilde{a}^{1:N}$  by inverting the empirical cumulative distribution function associated with these sorted samples, using common random numbers. We might sample  $a^k$  and  $\tilde{a}^k$  such that  $a^k \neq \tilde{a}^k$ , but  $a^k$  and  $\tilde{a}^k$  will still be close and thus  $x^{(a^k)}$  and  $\tilde{x}^{(\tilde{a}^k)}$  will be similar, thanks to the sorting. The method can be extended to multivariate spaces using the Hilbert space-filling curve as mentioned in [Deligiannidis et al. \(2015\)](#), following [Gerber and Chopin \(2015\)](#). That is, we use the pseudo-inverse of the Hilbert curve to map the  $d_x$ -dimensional particles to the interval  $[0, 1]$ , where they can be sorted in increasing order. We refer to this approach as sorted resampling, and use the implementation provided by the function `hilbert_sort` in [The CGAL Project \(2016\)](#). The cost of sorted resampling is of order  $N \log N$ .

## 2.6 Numerical illustration

We first illustrate the effect of coupled resampling schemes in estimating likelihood curves for a multivariate hidden auto-regressive model. The process starts as  $x_0 \sim \mathcal{N}(0, I_{d_x})$ , where  $I_{d_x}$  is the identity matrix of dimension  $d_x \times d_x$ , the transition is defined by  $x_t \sim \mathcal{N}(Ax_{t-1}, I_{d_x})$ , where  $A^{ij}$  is  $\theta^{|i-j|+1}$ , as in [Guarniero et al. \(2015\)](#). Finally, the measurement distribution is defined by  $y_t \sim \mathcal{N}(x_t, I_{d_x})$ .

We generate  $T = 1,000$  observations, with parameter  $\theta = 0.4$  and with  $d_x = 5$ . We consider a sequence of parameter values  $\theta_1, \dots, \theta_L$ . We run a standard particle filter given  $\theta_1$ , and then for each  $\ell \in 2 : L$ , we run a particle filter given  $\theta_\ell$  conditionally upon the variables generated by the previous particle filter given  $\theta_{\ell-1}$ ; more details are given in [Appendix A](#). We use  $N = 128$  particles, and try various coupled resampling schemes. The transport resampling scheme uses  $\varepsilon = 0.01 \times \text{median}(D)$  and  $\alpha = 0.99$ . The estimated log-likelihoods are shown in [Figure 1](#) for five independent runs, and compared to the exact log-likelihood obtained by Kalman filters.

All the filters under-estimate the log-likelihood by a significant amount, indicating that more particles would be necessary to obtain precise estimates for any given  $\theta$ . However, we see that



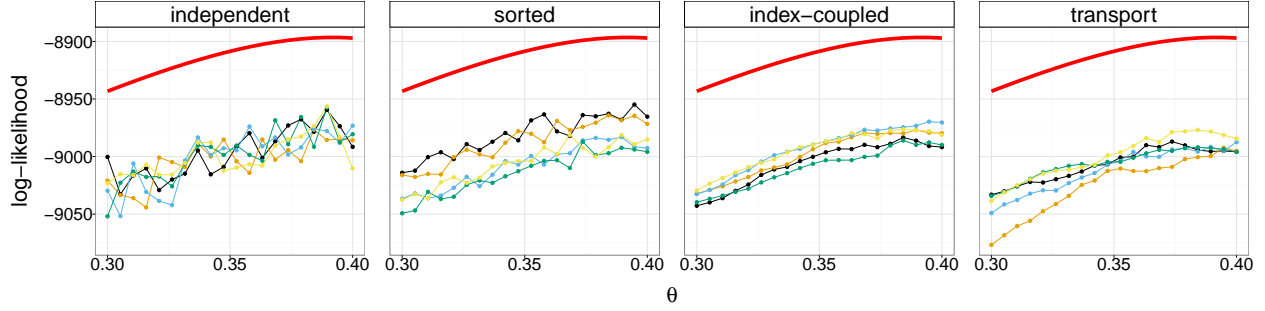


Figure 1: Log-likelihood estimators for various values of  $\theta$  in a hidden auto-regressive model with  $d_x = 5$ ,  $T = 1,000$  and  $N = 128$ . From left to right: independent estimators, common random numbers with sorted resampling, with index-coupled resampling and with transport resampling. The thick red line indicates the exact log-likelihood computed using Kalman filters.

the shape of the log-likelihood curve is still approximately recovered when using common random numbers and certain coupled resampling schemes, indicating that we can compare log-likelihood values for different parameters, even with comparably small numbers of particles.

### 3 Methodological developments using coupled resampling

In this section, we develop the use of coupled resampling schemes for score estimation, for sampling algorithms targeting the posterior distribution of the parameters, and for latent state estimation. For the latter, a new smoother is proposed, conditions for its validity are given and experiments in a toy example are presented, showing its potential advantages compared to standard smoothing methods.

#### 3.1 Finite difference estimators of the score

Consider the estimation of the log-likelihood gradient, also called the score and denoted by  $\nabla_{\theta} \log p(y_{1:T}|\theta)$ . We focus on univariate parameters for simplicity. A finite difference estimator (Asmussen and Glynn, 2007) of the score at the value  $\theta$  is given by  $D_h^N(\theta) = (\log \hat{p}^N(y_{1:T}|\theta + h) - \log \hat{p}^N(y_{1:T}|\theta - h))/(2h)$ , where  $h > 0$  is a perturbation parameter. If  $h$  is small, the variances of the two log-likelihood estimators can be assumed approximately equal, and thus  $\mathbb{V}(D_h^N(\theta))$  is approximately equal to  $(2h)^{-1} \times \mathbb{V}(\log \hat{p}^N(y_{1:T}|\theta)) \times (1 - \rho_h^N(\theta))$ , where  $\rho_h^N(\theta)$  denotes the correlation between  $\log \hat{p}^N(y_{1:T}|\theta + h)$  and  $\log \hat{p}^N(y_{1:T}|\theta - h)$ . Thus, compared to using independent estimators with the same variance, the variance of the finite difference estimator can be divided by  $1/(1 - \rho_h^N(\theta))$ . We refer to this number as the gain. It corresponds to how many times more particles should be used in order to attain the same accuracy using independent particle filters. The bias of the gradient estimator is unchanged by the use of coupled resampling schemes, since they do not change the marginal distributions of each particle filter.



Figure 2: Correlation (rounded to two decimals) and gain (variance reduction) factors, as a function of the perturbation parameter  $h$ , in a five-dimensional hidden auto-regressive model with  $T = 1,000$ ,  $N = 128$  and  $R = 1,000$  experiments.

h	method	correlation	gain
0.001	sorted	0.90	9.6
0.001	index-coupled	1.00	527.5
0.001	transport	1.00	321.7
0.025	sorted	0.88	8.3
0.025	index-coupled	0.96	25.2
0.025	transport	0.97	33.0
0.05	sorted	0.84	6.2
0.05	index-coupled	0.91	11.1
0.05	transport	0.92	12.7

We run coupled particle filters at  $\theta - h$  and  $\theta + h$  for  $\theta = 0.3$  and various  $h$ , and different coupled resampling schemes, over 1,000 independent experiments in the hidden auto-regressive model of Section 2.6. The correlations between the log-likelihood estimators are shown in Figure 2, as well as the gains. We see that the variance can be divided by approximately 500 for small values of  $h$ , but only by approximately 10 for larger values of  $h$ . Index-coupled resampling appears to perform better than transport resampling for small values of  $h$ , perhaps due to the approximation introduced in the regularized transport problem; a more detailed investigation of the transport regularization is given in the next section. Here the tuning parameters of transport resampling were set to  $\varepsilon = 5\% \times \text{median}(D)$  and  $\alpha = 99\%$ .

### 3.2 Correlated particle marginal Metropolis–Hastings

We now turn to the particle marginal MH algorithm (PMMH) (Andrieu et al., 2010), for parameter inference in state space models. Denoting the prior parameter distribution by  $p(d\theta)$ , the algorithm generates a Markov chain  $(\theta^{(i)})_{i \geq 1}$  targeting the posterior distribution  $p(d\theta|y_{1:T}) \propto p(d\theta)p(y_{1:T}|\theta)$ . At iteration  $i \geq 1$ , a parameter  $\tilde{\theta}$  is proposed from a Markov kernel  $q(d\theta|\theta^{(i-1)})$ , and accepted as the next state of the chain  $\theta^{(i)}$  with probability

$$\min \left( 1, \frac{\hat{p}^N(y_{1:T}|\tilde{\theta})}{\hat{p}^N(y_{1:T}|\theta^{(i-1)})} \frac{p(\tilde{\theta})}{p(\theta^{(i-1)})} \frac{q(\theta^{(i-1)}|\tilde{\theta})}{q(\tilde{\theta}|\theta^{(i-1)})} \right), \quad (2)$$

where  $\hat{p}^N(y_{1:T}|\tilde{\theta})$  is the likelihood estimator produced by a filter given  $\tilde{\theta}$ . In order for this algorithm to mimic the ideal underlying MH algorithm, the ratio of likelihood estimators must be an accurate approximation of the exact ratio of likelihoods (Andrieu and Vihola, 2015). The benefit of correlated likelihood estimators within pseudo-marginal algorithms is the topic of recent works (Deligiannidis et al., 2015; Dahlin et al., 2015), following Lee and Holmes (2010) in the discussion of Andrieu

et al. (2010).

A correlated particle marginal MH algorithm works on the joint space of the parameter  $\theta$ , the process-generating variables  $\mathbf{U}_t$  for all  $t \in 0 : T$ , and the ancestor variables  $\mathbf{a}_t$ , for all  $t \in 0 : T - 1$ . Denote by  $\varphi$  the distribution of  $\mathbf{U}_{0:T}$ , assumed to be standard multivariate normal for simplicity, and let  $\phi$  be a Markov kernel leaving  $\varphi$  invariant. Consider any iteration  $i \geq 1$  of the algorithm; the current state of the Markov chain contains  $\theta^{(i-1)} = \theta$ ,  $\mathbf{U}_{0:T}^{(i-1)} = \mathbf{U}_{0:T}$ ,  $\mathbf{a}_{0:T-1}^{(i-1)} = \mathbf{a}_{0:T-1}$ , and the associated likelihood estimator is  $\hat{p}^N(y_{1:T}|\theta)$ . The particles  $(\mathbf{w}_t, \mathbf{x}_t)$ , for all  $t \in 0 : T$ , are deterministic given  $\theta$ ,  $\mathbf{U}_{0:T}$  and  $\mathbf{a}_{0:T-1}$ . The algorithm proceeds in the following way.

1. A parameter value is proposed:  $\tilde{\theta} \sim q(d\tilde{\theta}|\theta)$ , as well as new process-generating variables:  $\tilde{\mathbf{U}}_{0:T} \sim \phi(d\tilde{\mathbf{U}}_{0:T}|\mathbf{U}_{0:T})$ .
2. A particle filter is run given  $\tilde{\theta}$ , using  $\tilde{\mathbf{U}}_{0:T}$  and conditionally upon the current particle filter. That is, at each resampling step, a matrix  $P_t$  is computed using  $(\mathbf{w}_t, \mathbf{x}_t)$  and  $(\tilde{\mathbf{w}}_t, \tilde{\mathbf{x}}_t)$ , and the new ancestors  $\tilde{\mathbf{a}}_t$  are sampled conditional upon  $\mathbf{a}_t$ . The algorithm produces ancestor variables  $\tilde{\mathbf{a}}_{0:T-1}$  and a likelihood estimator  $\hat{p}^N(y_{1:T}|\tilde{\theta})$ .
3. With the probability given by Eq. (2), the chain moves to the state with parameter  $\tilde{\theta}$ , variables  $\tilde{\mathbf{U}}_{0:T}$ , ancestors  $\tilde{\mathbf{a}}_{0:T-1}$  and likelihood estimator  $\hat{p}^N(y_{1:T}|\tilde{\theta})$ . Otherwise, the current state of the chain is unchanged.

Appendix A contains further details on the conditional sampling of a particle filter as required by step (b) above. Appendix B contains conditions on the coupled resampling scheme for the algorithm to be exact, which are verified for sorted and index-coupled schemes, as well as for a slightly modified transport scheme.

In the hidden auto-regressive model, we specify a standard normal prior on  $\theta$ . The distribution  $\varphi$  of the process-generating variables is a multivariate normal distribution, and we choose the kernel  $\phi$  to be auto-regressive:  $\tilde{\mathbf{U}} = \rho\mathbf{U} + \sqrt{1 - \rho^2}\mathcal{N}(0, I)$ , with  $\rho = 0.999$ . We use a normal random walk with a standard deviation of 0.01 for the proposal on  $\theta$ . We run each algorithm 100 times for  $M = 20,000$  iterations, starting the chain from a uniform variable in  $[0.37, 0.41]$ , taken to be in the bulk of the posterior distribution. Figure 3 shows the obtained average acceptance rates and effective sample sizes, defined as  $M$  divided by the integrated autocorrelation time and obtained with the function `effectiveSize` of the `coda` package. With index-coupled resampling, the effective sample size can reach acceptable levels with fewer particles, compared to standard PMMH or compared to sorted resampling (as used by Deligiannidis et al. (2015)).

Transport resampling is considerably more expensive for a given choice of  $N$ . For  $N = 128$ , we show the acceptance rates and effective sample sizes obtained over 20 independent experiments with various levels of approximation to the optimal transport problem. When  $\epsilon$  is close to zero and  $\alpha$  is close to one, we can achieve greater effective sample sizes with transport resampling than with the other schemes, for a fixed  $N$ .

Figure 3: Average acceptance rates (AR) and effective sample sizes (ESS) of standard and correlated PMMH, obtained for various numbers of particles (left), and for various regularization parameters  $\varepsilon$  and stopping criteria  $\alpha$  for the transport resampling scheme with  $N = 128$  (right), in a hidden auto-regressive model with  $d_x = 5$ ,  $T = 1,000$  and  $M = 20,000$  iterations.

N	method	AR (%)	ESS
64	indep.	0.06 (0.02)	29 (95)
64	sorted	0.12 (0.06)	25 (50)
64	index-c.	0.87 (0.23)	41 (16)
128	indep.	0.06 (0.02)	23 (41)
128	sorted	0.18 (0.10)	26 (28)
128	index-c.	2.00 (0.41)	98 (30)
256	indep.	0.07 (0.03)	16 (24)
256	sorted	0.42 (0.23)	39 (25)
256	index-c.	4.67 (0.49)	244 (58)

Standard PMMH (indep.), and with sorted and index-coupled resampling (index-c.), over 100 experiments.

$\varepsilon$	$\alpha$	AR (%)	ESS
0.10	0.95	1.06 (0.29)	83 (34)
0.10	0.99	1.12 (0.28)	85 (23)
0.05	0.95	2.13 (0.47)	133 (44)
0.05	0.99	3.86 (0.49)	220 (54)

With  $N = 128$  and transport resampling, over 20 experiments.

### 3.3 A new smoothing method

Next, we turn to an application of *coupled conditional particle filters* for the task of smoothing. The parameter  $\theta$  is fixed and removed from the notation. Denote by  $h$  a generic test function on  $\mathbb{X}^{T+1}$ , of which we want to compute the expectation with respect to the smoothing distribution  $\pi(dx_{0:T}) = p(dx_{0:T}|y_{1:T})$ ; we write  $\pi(h)$  for  $\int_{\mathbb{X}^{T+1}} h(x_{0:T})\pi(dx_{0:T})$ .

#### 3.3.1 Algorithm

We build upon the debiasing technique of Glynn and Rhee (2014), which follows a series of unbiased estimation techniques (see Rhee and Glynn, 2012; Vihola, 2015, and references therein). The Rhee–Glynn estimator introduced in Glynn and Rhee (2014) uses the kernel of a Markov chain with invariant distribution  $\pi$ , in order to produce unbiased estimators of  $\pi(h)$ . In the setting of smoothing, the conditional particle filter defines a Markov kernel leaving the smoothing distribution invariant Andrieu et al. (2010); extensions include backward sampling (Whiteley, 2010) and ancestor sampling (Lindsten et al., 2014). The conditional particle filter kernel has been extensively studied in Chopin and Singh (2015); Andrieu et al. (2013); Lindsten et al. (2015). The use of conditional particle filters within the Rhee–Glynn estimator naturally leads to the problem of coupling two conditional particle filters.

The Rhee–Glynn construction adapted to our context goes as follows. We draw two trajectories  $X^{(0)}$  and  $\tilde{X}^{(0)}$  from two independent particle filters, which we denote by  $X^{(0)} \sim \text{PF}(\mathbf{U}^{(0)})$  and  $\tilde{X}^{(0)} \sim \text{PF}(\tilde{\mathbf{U}}^{(0)})$ , with  $\mathbf{U}^{(0)} \sim \varphi$  and  $\tilde{\mathbf{U}}^{(0)} \sim \varphi$  denoting the process-generating variables. Note

---

**Algorithm 1** Rhee–Glynn smoothing estimator.

---

- Draw  $\mathbf{U}^{(0)} \sim \varphi$  and  $X^{(0)} \sim \text{PF}(\mathbf{U}^{(0)})$ , draw  $\mathbf{U}^{(1)} \sim \varphi$ , and draw  $X^{(1)} \sim \text{CPF}(X^{(0)}, \mathbf{U}^{(1)})$ .
  - Draw  $\tilde{\mathbf{U}}^{(0)} \sim \varphi$  and  $\tilde{X}^{(0)} \sim \text{PF}(\tilde{\mathbf{U}}^{(0)})$ .
  - Compute  $\Delta^{(0)} = h(X^{(0)})$  and  $\Delta^{(1)} = h(X^{(1)}) - h(\tilde{X}^{(0)})$ , set  $H = \Delta^{(0)} + \Delta^{(1)}$ .
  - For  $n = 2, 3, \dots$ ,
    - Draw  $\mathbf{U}^{(n)} \sim \varphi$  and  $(X^{(n)}, \tilde{X}^{(n-1)}) \sim \text{CCPF}(X^{(n-1)}, \tilde{X}^{(n-2)}, \mathbf{U}^{(n)})$ .
    - Compute  $\Delta^{(n)} = h(X^{(n)}) - h(\tilde{X}^{(n-1)})$ , set  $H \leftarrow H + \Delta^{(n)}$ .
    - If  $X^{(n)} = \tilde{X}^{(n-1)}$ , then  $n$  is the meeting time  $\tau$ : exit the loop.
  - Return  $H$ .
- 

that even for fixed process-generating variables the sampled trajectories are random, due to the randomness of the resampling steps. We apply one step of the conditional particle filter to the first trajectory: we sample process-generating variables  $\mathbf{U}^{(1)} \sim \varphi$  and write  $X^{(1)} \sim \text{CPF}(X^{(0)}, \mathbf{U}^{(1)})$ . Then, for all  $n \geq 2$ , we apply the coupled conditional particle filter (CCPF) to the pair of trajectories, which is written  $(X^{(n)}, \tilde{X}^{(n-1)}) \sim \text{CCPF}(X^{(n-1)}, \tilde{X}^{(n-2)}, \mathbf{U}^{(n)})$ , where  $\mathbf{U}^{(n)} \sim \varphi$ . The resulting chains are such that

1. marginally,  $(X^{(n)})_{n \geq 0}$  and  $(\tilde{X}^{(n)})_{n \geq 0}$  have the same distributions as if they were generated by conditional particle filters, and thus converge under mild assumptions to the smoothing distribution;
2. for each  $n \geq 0$ ,  $X^{(n)}$  has the same distribution as  $\tilde{X}^{(n)}$ , since the variables  $(\mathbf{U}^{(n)})_{n \geq 0}$  are independent and identically distributed;
3. under mild conditions stated below, at each iteration  $n \geq 2$ , there is a non-zero probability that  $X^{(n)} = \tilde{X}^{(n-1)}$ . We refer to this event as a meeting, and introduce the meeting time  $\tau$ , defined as  $\tau = \inf\{n \geq 2 : X^{(n)} = \tilde{X}^{(n-1)}\}$ .

We then define the Rhee–Glynn smoothing estimator as

$$H = h(X^{(0)}) + \sum_{n=1}^{\tau} h(X^{(n)}) - h(\tilde{X}^{(n-1)}). \quad (3)$$

This is an unbiased estimator of  $\pi(h)$  with finite variance and finite computational cost, under conditions given below. The full procedure is described in Algorithm 1. To estimate the smoothing functional  $\pi(h)$ , one can sample  $R$  estimators,  $H^{(r)}$  for  $r \in 1 : R$ , and take the empirical average  $\bar{H} = R^{-1} \sum_{r=1}^R H^{(r)}$ ; it is unbiased and converges to  $\pi(h)$  at the standard Monte Carlo rate as  $R \rightarrow \infty$ .

Popular smoothing techniques include the fixed-lag smoother and the forward filtering backward smoother (see [Doucet and Johansen, 2011](#); [Lindsten and Schön, 2013](#); [Kantas et al., 2015](#), for recent reviews). The Rhee–Glynn smoothing estimator sets itself apart in the following way, due to its form as an average of independent unbiased estimators.

1. Complete parallelization of the computation of the terms  $H^{(r)}$  is possible. On the contrary, particle-based methods are not entirely parallelizable due to the resampling step ([Murray et al., 2015](#); [Lee and Whiteley, 2015a](#)).
2. Error estimators can be constructed based on the central limit theorem, allowing for an empirical assessment of the performance of the estimator. Error estimators for particle smoothers have not yet been proposed, although see [Lee and Whiteley \(2015b\)](#).

### 3.3.2 Theoretical properties

We give three sufficient conditions for the validity of Rhee–Glynn smoothing estimators.

**Assumption 1.** The measurement density of the model is bounded from above:

$$\exists \bar{g} < \infty, \quad \forall y \in \mathbb{Y}, \quad \forall x \in \mathbb{X}, \quad g(y|x, \theta) \leq \bar{g}.$$

That bound limits the influence of the reference trajectory in the conditional particle filter.

**Assumption 2.** The resampling probability matrix  $P$ , constructed from the weight vectors  $\mathbf{w}$  and  $\tilde{\mathbf{w}}$ , is such that

$$\forall i \in \{1, \dots, N\}, \quad P^{ii} \geq w^i \tilde{w}^i.$$

Furthermore, if  $\mathbf{w} = \tilde{\mathbf{w}}$ , then  $P$  is a diagonal matrix with entries given by  $\mathbf{w}$ .

One can check that the condition holds for independent and index-coupled resampling schemes. The second part of Assumption 2 ensures that if two reference trajectories are equal, an application of the coupled conditional particle filter returns two identical trajectories.

**Assumption 3.** Let  $(X^{(n)})_{n \geq 0}$  be a Markov chain generated by the conditional particle filter. The test function  $h$  is such that

$$\mathbb{E} \left[ h(X^{(n)}) \right] \xrightarrow{n \rightarrow \infty} \pi(h).$$

Furthermore, there exists  $\delta > 0$ ,  $n_0 < \infty$  and  $C < \infty$  such that

$$\forall n \geq n_0, \quad \mathbb{E} \left[ h(X^{(n)})^{2+\delta} \right] \leq C.$$

This assumption relates to the validity of the conditional particle filter to estimate  $\pi(h)$ , addressed under general assumptions in [Chopin and Singh \(2015\)](#); [Andrieu et al. \(2013\)](#); [Lindsten](#)

et al. (2015). Up to the term  $\delta > 0$  which can be arbitrarily small, the assumption is a requirement if we want to estimate  $\pi(h)$  using conditional particle filters while ensuring a finite variance.

Our main result states that the proposed estimator is unbiased and has a finite variance. Similar results can be found in Theorem 1 in Rhee (2013), Theorem 2.1 in McLeish (2012), Theorem 7 in Vihola (2015) and in Glynn and Rhee (2014).

**Theorem 3.1.** Under Assumptions 1-2-3, the Rhee–Glynn smoothing estimator  $H$ , given in Eq. (3), is an unbiased estimator of  $\pi(h)$  with

$$\mathbb{E}[H^2] = \sum_{n=0}^{\infty} \mathbb{E}[(\Delta^{(n)})^2] + 2 \sum_{n=0}^{\infty} \sum_{\ell=n+1}^{\infty} \mathbb{E}[\Delta^{(n)} \Delta^{(\ell)}] < \infty,$$

where  $\Delta^{(0)} = h(X^{(0)})$  and for  $n \geq 1$ ,  $\Delta^{(n)} = h(X^{(n)}) - h(\tilde{X}^{(n-1)})$ .

The proof is given in Appendix C. The theorem uses univariate notation for  $H$  and  $\Delta_n$ , but the Rhee–Glynn smoother can be applied to estimate multivariate smoothing functionals, for which the theorem can be interpreted component-wise.

### 3.3.3 Practical considerations

For a fixed computational budget, the only tuning parameter is the number of particles  $N$ , which implicitly sets the number of independent estimators  $R$  that can be obtained within the budget. The computational cost of producing an unbiased estimator  $H$  is of order  $NT \times \mathbb{E}[\tau]$ , and the expectation of  $\tau$  is seen empirically to decrease with  $N$ , so that the choice of  $N$  is not obvious; in practice we recommend choosing a value of  $N$  large enough so that the meeting time occurs within a few steps, but other considerations such as memory cost could be taken into account. The memory cost for each estimator is of order  $T + N \log N$  in average (Jacob et al., 2015). This memory cost holds also when using ancestor sampling (Lindsten et al., 2014), whereas backward sampling (Whiteley, 2010) results in a memory cost of  $NT$ . As in Glynn and Rhee (2014), we can appeal to Glynn and Whitt (1992) to obtain a central limit theorem parameterized by the computational budget instead of the number of samples.

The performance of the proposed estimator is tied to the meeting time. As in Chopin and Singh (2015), the coupling inequality (Lindvall, 2002) can be used to relate the meeting time with the mixing of the underlying conditional particle filter kernel. Thus, the proposed estimator is expected to work in the same situations where the conditional particle filter works. It can be seen as a framework to parallelize conditional particle filters and to obtain reliable confidence intervals. Furthermore, any improvement in the conditional particle filter directly translates into a more efficient Rhee–Glynn estimator.

The variance of the proposed estimator can first be reduced by a Rao–Blackwellization argument. In the  $n$ -th term of the sum in Eq. (3), the random variable  $h(X^{(n)})$  is obtained by applying

the test function  $h$  to a trajectory drawn among  $N$  trajectories, say  $x_{0:T}^{1:N}$ , with probabilities  $w_T^{1:N}$ . Thus the random variable  $\sum_{k=1}^N w_T^k h(x_{0:T}^k)$  is a conditional expectation of  $h(X^{(n)})$  given  $x_{0:T}^{1:N}$  and  $w_T^{1:N}$ , which has the same expectation as  $h(X^{(n)})$ . Any term  $h(X^{(n)})$  or  $h(\tilde{X}^{(n)})$  in  $H$  can be replaced by similar conditional expectations. This enables the use of all the particles generated by the conditional particle filters. A further variance reduction technique is discussed in Appendix D.

### 3.3.4 A hidden auto-regressive model with an unlikely observation

We consider the first example of Ruiz and Kappen (2016). The latent process is defined as  $x_0 \sim \mathcal{N}(0, \tau_0^2)$  and  $x_t = \eta x_{t-1} + \mathcal{N}(0, \tau^2)$ ; we take  $\tau_0 = 0.1$ ,  $\eta = 0.9$  and  $\tau = 0.1$  and consider  $T = 10$  time steps. The process is observed only at time  $T$ , where  $y_T = 1$  and we assume  $y_T \sim \mathcal{N}(x_T, \sigma^2)$ , with  $\sigma = 0.1$ . The observation  $y_T$  is unlikely under the latent process distribution. Therefore the filtering distributions and the smoothing distributions have little overlap, particular for times  $t$  close to  $T$ .

We consider the problem of estimating the smoothing means, and run  $R = 10,000$  independent Rhee–Glynn estimators, with various numbers of particles, with ancestor sampling (Lindsten et al., 2014) and without variance reduction. For comparison, we also run a bootstrap particle filter  $R$  times, with larger numbers of particles. This compensates for the fact that the Rhee–Glynn estimator requires a certain number of iterations, each involving a coupled particle filter. The average meeting times for each value of  $N$  are: 10.6 (25.1) for  $N = 128$ , 8.9 (17.0) for  $N = 256$ , 7.3 (10.8) for  $N = 512$ , 6.1 (7.3) for  $N = 1024$ .

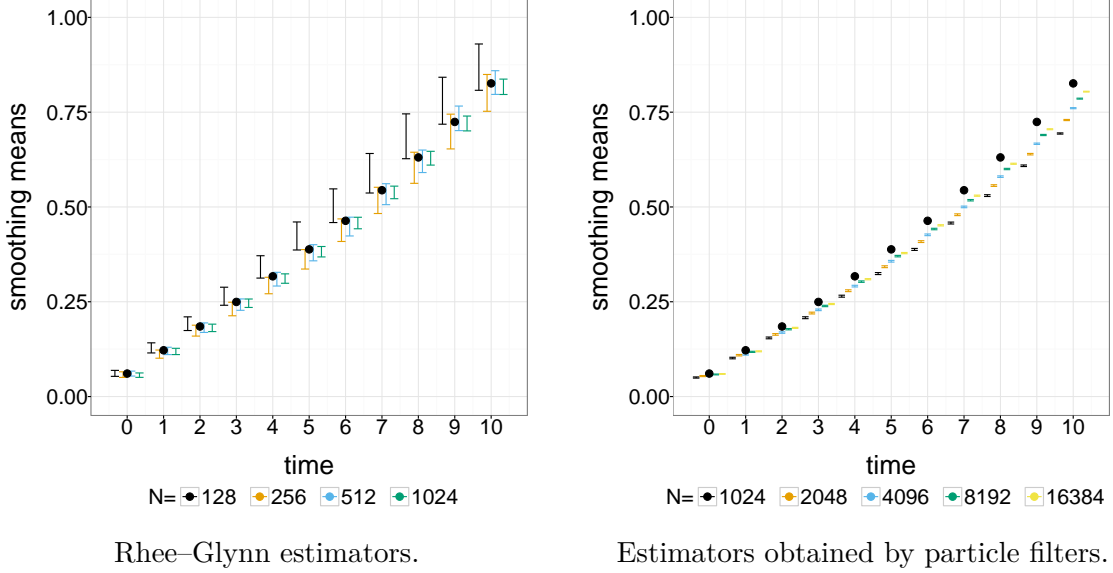
For each method, we compute a confidence interval as  $[\hat{x}_t - 2\hat{\sigma}_t/\sqrt{R}, \hat{x}_t + 2\hat{\sigma}_t/\sqrt{R}]$  at each time  $t$ , where  $\hat{x}_t$  is the mean of the  $R$  estimators and  $\hat{\sigma}_t$  is the standard deviation. The results are shown in Figure 4. The exact smoothing means are obtained analytically and shown by black dots. The Rhee–Glynn estimators lead to reliable confidence intervals. Increasing  $N$  reduces the width of the interval and the average meeting time. On the other hand, standard particle smoothers with larger numbers of particles still yield unreliable confidence intervals. The poor performance of standard particle smoothers is to be expected in the setting of highly-informative observations (Ruiz and Kappen, 2016; Del Moral and Murray, 2015).

## 4 Numerical experiments in a prey-predator model

We investigate the performance of the correlated particle marginal Metropolis–Hastings algorithm and of the Rhee–Glynn smoother for a nonlinear non-Gaussian model. We consider the Plankton–Zooplankton model of Jones et al. (2010), which is an example of an implicit model: the transition density is intractable (Bretó et al., 2009; Jacob, 2015). The hidden state  $x_t = (p_t, z_t)$  represents the population size of phytoplankton and zooplankton, and the transition from time  $t$  to  $t + 1$  is



Figure 4: Confidence intervals on the smoothing means, obtained with  $R = 10,000$  Rhee–Glynn smoothers (left), and bootstrap particle filters (right). The true smoothing means are shown using black dots. (Note that the estimators for different times are dependent since they are obtained from the same trajectories.)



given by a Lotka–Volterra equation,

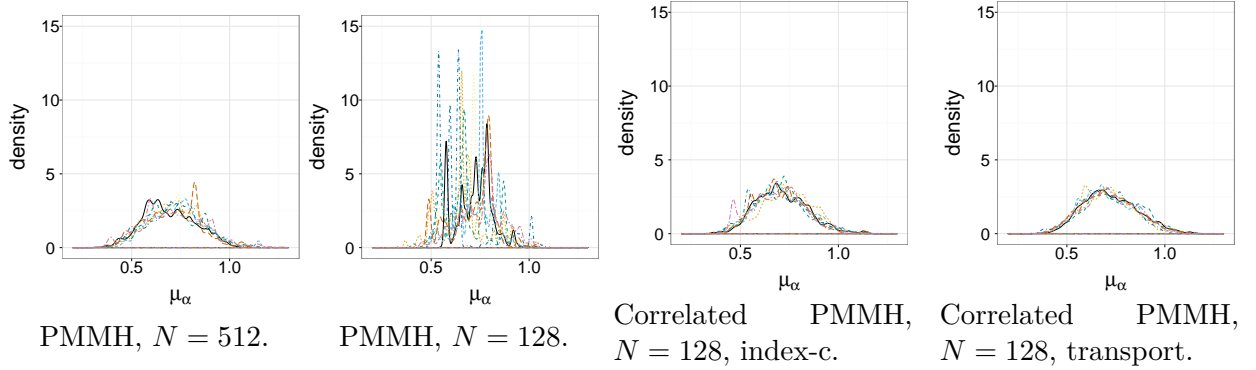
$$\frac{dp_t}{dt} = \alpha p_t - c p_t z_t, \quad \text{and} \quad \frac{dz_t}{dt} = e c p_t z_t - m_l z_t - m_q z_t^2,$$

where the stochastic daily growth rate  $\alpha$  is drawn from  $\mathcal{N}(\mu_\alpha, \sigma_\alpha^2)$  at every integer time  $t$ . The propagation of each particle involves solving numerically the above equation, here using a Runge–Kutta method in the `odeint` library (Ahnert and Mulansky, 2011). The initial distribution is given by  $\log p_0 \sim \mathcal{N}(\log 2, 1)$  and  $\log z_0 \sim \mathcal{N}(\log 2, 1)$ . The parameters  $c$  and  $e$  represent the clearance rate of the prey and the growth efficiency of the predator. Both  $m_l$  and  $m_q$  parameterize the mortality rate of the predator. The observations  $y_t$  are noisy measurements of the phytoplankton  $p_t$ ,  $\log y_t \sim \mathcal{N}(\log p_t, 0.2^2)$ ;  $z_t$  is not observed. We generate  $T = 365$  observations using  $\mu_\alpha = 0.7, \sigma_\alpha = 0.5, c = 0.25, e = 0.3, m_l = 0.1, m_q = 0.1$ .

#### 4.1 Correlated particle marginal Metropolis–Hastings

The parameter is  $\theta = (\mu_\alpha, \sigma_\alpha, c, e, m_l, m_q)$ . We specify a centered normal prior on  $\mu_\alpha$  with variance 100, an exponential prior on  $\sigma_\alpha$  with unit rate, and uniform priors in  $[0, 1]$  for the four other parameters. With logarithm and logistic transforms, we map  $\theta$  to  $\mathbb{R}^6$ . For the Metropolis–Hastings proposal distribution, we use a normal random walk with a covariance matrix chosen as one sixth of the covariance of the posterior, obtained from long pilot runs. We start the Markov chains at the

Figure 5: Density plots obtained with standard PMMH with  $N = 1,024$  (left), with  $N = 128$  (middle left), and with correlated PMMH with  $N = 128$  and index-coupled resampling (middle right) and transport resampling (right), for the parameter  $\mu_\alpha$  of the phytoplankton–zooplankton model with  $T = 365$  observations. The results from 10 independent experiments with  $M = 100,000$  iterations are overlaid.



(transformed) data-generating parameter. We then run the particle marginal Metropolis–Hastings with  $N = 512$  particles and  $M = 100,000$  iterations, 10 times independently, and obtain a mean acceptance rate of 4.5%, with standard deviation of 0.3%, and an effective sample size averaged over the parameters (ESS) of 106 (54). With only  $N = 128$  particles, we obtain a mean acceptance of 0.4% (0.1%) and an ESS of 19 (10). Density estimators of the posterior of  $\mu_\alpha$  with these two samplers are shown on the left-most plots of Figure 5.

We investigate whether we can obtain better posterior approximations using the correlated Metropolis–Hastings algorithm, still with  $N = 128$  particles and  $M = 100,000$  iterations. We set the correlation coefficient for the propagation of the process-generating variables to  $\rho = 0.99$ . We consider the use of index-coupled, sorted and transport resampling. For the latter we choose  $\varepsilon = 0.1 \times \text{median}(D)$  and  $\alpha = 0.95$ . For index-coupled resampling, we obtain an acceptance of 4.2% (0.5%), with sorted resampling 5.0% (0.5%) and with transport resampling 5.4% (0.4%). For the ESS, we obtain 108 (45) for index-coupled resampling, 113 (61) for sorted resampling and 117 (53) for transport resampling. We display the density estimators of the posterior of  $\mu_\alpha$  in the right-most panels of Figure 5, for index-coupled and transport resampling. Similar results are obtained with sorted resampling (not shown). However, results in Section 3.2 indicate that sorted resampling would be less efficient in higher dimension. We conclude that the correlated algorithm with  $N = 128$  particles give posterior approximations that are comparable to those obtained with a standard PMMH algorithm that uses four times more particles; thus important computational savings can be made. With the provided R implementation, the algorithm with  $N = 128$  and transport resampling takes around 1000 minutes per run, compared to 200 minutes for the other schemes, and around 700 minutes for the standard algorithm with  $N = 512$ .

## 4.2 Rhee–Glynn smoother

Next, we consider the problem of estimating the mean population of zooplankton at each time  $t \in 0 : T$ , given a fixed parameter taken to be the data-generating one. The intractability of the transition density precludes the use of ancestor or backward sampling, or the use of forward filtering backward sampling.

We draw  $R = 1,000$  independent Rhee–Glynn smoothing estimators, using  $N = 4,096$  particles. The observed meeting times have a median of 4, a mean of 4.7 and a maximum of 19. The estimator  $\hat{z}_t$  of the smoothing mean of  $z_t$  at each time  $t$  is obtained by averaging  $R = 1,000$  independent estimators. We compute the Monte Carlo variance  $\hat{v}_t$  of  $\hat{z}_t$  at each time, and define the relative variance as  $\hat{v}_t/(\hat{z}_t^2)$ .

We combine the Rhee–Glynn estimator (denoted by “unbiased” below) with the variance reduction technique of Section 3.3.3 (denoted by “unbiased+RB”). Furthermore, we use the variance reduction of Appendix D, denoted by “unbiased+RB+m”, with  $m$  chosen to be the median of the meeting time, i.e.  $m = 4$ . The latter increases the average meeting time from 4.7 to 5.1. We compare the resulting estimators with a fixed-lag smoother (Doucet and Johansen, 2011) with a lag parameter  $L = 10$ , and with a standard particle filter storing the complete trajectories.

We use the same number of particles  $N = 4,096$  and compute  $R = 1,000$  estimators for each method. The relative variance is shown in Figure 6. First we see that the variance reduction techniques have a significant effect, particularly for  $t$  close to  $T$  but also for small  $t$ . In particular, the estimator  $H_{m,\infty}$  with Rao–Blackwellization (“unbiased+RB+m”) achieves nearly the same relative variance as the particle filter. The cost of these estimators can be computed as the number of iterations  $\max(m, \tau)$ , times twice the cost of a particle filter for each coupled particle filter. In the present setting where the average number of iterations is around five, we conclude that removing the bias from the standard particle filter can be done for an approximate ten-fold increase in computational cost. As expected the fixed-lag smoother leads to a significant decrease in variance. For this model, the incurred bias is negligible for  $L = 10$  (not shown), which, however, would be hard to tell if we did not have access to either unbiased methods or long runs of asymptotically exact methods.

In this model, standard particle filters and fixed-lag approximations perform well, leading to smaller mean squared error than the proposed estimators, for a given computational cost. However, the proposed estimators are competitive, the tuning of the algorithm is minimal, and unbiasedness prevents the possibility of over-confident error bars as in Section 3.3.4. Therefore the proposed method trades an extra cost for convenience and reliability.

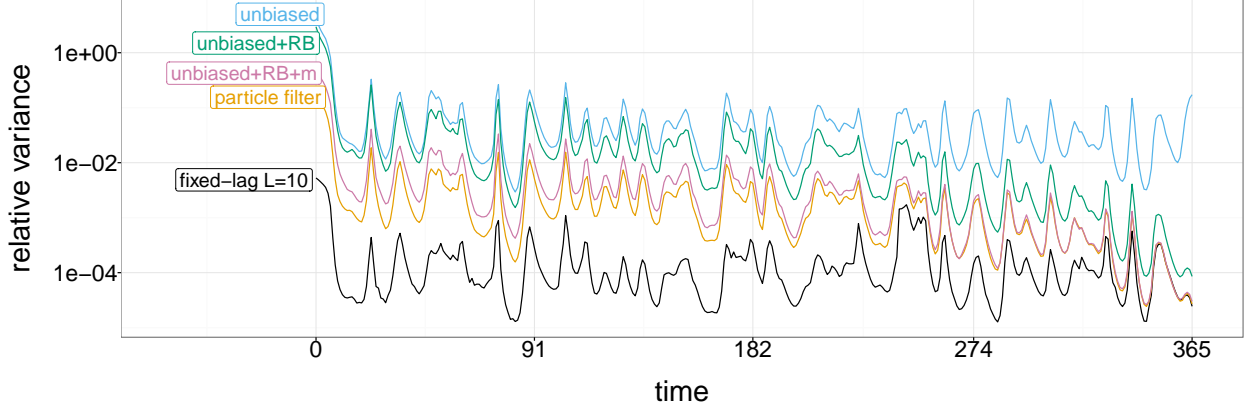


Figure 6: Comparison of the relative variance of the standard particle filter, a fixed-lag smoother with lag  $L = 10$ , and the proposed unbiased method, with Rao–Blackwellization (RB) and variance reduction (RB+m), for the estimation of the mean of the zooplankton population  $z_t$ , for the phytoplankton–zooplankton model with  $T = 365$  observations.

## 5 Discussion

Coupled particle filters can be beneficial in multiple settings. Coupled bootstrap particle filters can be helpful in score estimation and parameter inference, while coupled conditional particle filters lead to a new smoothing algorithm. The attractive features of the Rhee–Glynn smoother include simple parallelization and accurate error bars; these traits would be shared by perfect samplers, which aim at the more ambitious task of sampling exactly from the smoothing distribution (Lee et al., 2014).

We have shown the validity of the Rhee–Glynn estimator under mild conditions, and its behaviour as a function of the time horizon and the number of particles deserves further analysis. Numerical experiments in Appendix F investigate the effect of the time horizon and of the number of particles, among other effects. Furthermore, together with Fisher’s identity (Poyiadjis et al., 2011), the proposed smoother produces unbiased estimators of the score, for models where the transition density is tractable. This could in turn help maximizing the likelihood via stochastic gradients.

Another topic of future research might be the development of coupling ideas outside the context of state space models, following the growing popularity of particle methods in varied settings (see e.g. Del Moral et al., 2006; Bouchard-Côté et al., 2012; Naesseth et al., 2014).

### Appendices

Appendix A describes the sampling of a second particle filter given a first one. Appendix B provides conditions for the validity of the correlated particle marginal Metropolis–Hastings, and Appendix C for the validity of the Rhee–Glynn smoother. Appendix D describes an additional variance reduction technique for the Rhee–Glynn smoother. Appendix E provides a description of

the approximation of the transport problem. Appendix F provides extensive numerical experiments for the proposed smoother and Appendix G gives pseudo-code descriptions. R functions to reproduce the figures of the article are provided at [github.com/pierrejacob/](https://github.com/pierrejacob/) in CoupledPF and CoupledCPF.

## Acknowledgements

Similar ideas and other applications of coupled resampling schemes have been independently proposed in Sen et al. (2016). The first author thanks Mathieu Gerber and Marco Cuturi for helpful discussions. This work was initiated during the workshop on *Advanced Monte Carlo methods for complex inference problems* at the Isaac Newton Institute for Mathematical Sciences, Cambridge, UK held in April 2014. We would like to thank the organizers for a great event which led to this work.

## References

- Ahnert, K. and Mulansky, M. (2011) Odeint-solving ordinary differential equations in C++. *arXiv preprint arXiv:1110.3397*.
- Andrieu, C., Doucet, A. and Holenstein, R. (2010) Particle Markov chain Monte Carlo (with discussion). *Journal of the Royal Statistical Society: Series B (Statistical Methodology)*, **72**, 357–385.
- Andrieu, C., Lee, A. and Vihola, M. (2013) Uniform ergodicity of the iterated conditional SMC and geometric ergodicity of particle Gibbs samplers. *arXiv preprint arXiv:1312.6432*.
- Andrieu, C. and Vihola, M. (2015) Convergence properties of pseudo-marginal Markov chain Monte Carlo algorithms. *The Annals of Applied Probability*, **25**, 1030–1077.
- Asmussen, S. and Glynn, P. W. (2007) *Stochastic simulation: Algorithms and analysis*, vol. 57. Springer.
- Aude, G., Cuturi, M., Peyré, G. and Bach, F. (2016) Stochastic optimization for large-scale optimal transport. *arXiv preprint arXiv:1605.08527*.
- Benamou, J.-D., Carlier, G., Cuturi, M., Nenna, L. and Peyré, G. (2015) Iterative Bregman projections for regularized transportation problems. *SIAM Journal on Scientific Computing*, **37**, A1111–A1138.
- Bérard, J., Del Moral, P. and Doucet, A. (2014) A lognormal central limit theorem for particle approximations of normalizing constants. *Electron. J. Probab*, **19**, 1–28.
- Bouchard-Côté, A., Sankararaman, S. and Jordan, M. I. (2012) Phylogenetic inference via sequential Monte Carlo. *Systematic Biology*, **61**, 579–593.

- Bretó, C., He, D., Ionides, E. L. and King, A. A. (2009) Time series analysis via mechanistic models. *The Annals of Applied Statistics*, 319–348.
- Cappé, O., Moulines, E. and Rydén, T. (2005) *Inference in Hidden Markov Models*. Springer-Verlag, New York.
- Cérou, F., Del Moral, P. and Guyader, A. (2011) A nonasymptotic theorem for unnormalized Feynman–Kac particle models. *Ann. Inst. Henri Poincaré*, **47**, 629–649.
- Chopin, N. and Singh, S. S. (2015) On particle Gibbs sampling. *Bernoulli*, **21**, 1855–1883.
- Cuturi, M. (2013) Sinkhorn distances: Lightspeed computation of optimal transport. In *Advances in Neural Information Processing Systems (NIPS)*, 2292–2300.
- Cuturi, M. and Doucet, A. (2014) Fast computation of Wasserstein barycenters. In *Proceedings of the 31st International Conference on Machine Learning (ICML)*, 685–693.
- Dahlin, J., Lindsten, F., Kronander, J. and Schön, T. B. (2015) Accelerating pseudo-marginal Metropolis–Hastings by correlating auxiliary variables. *arXiv preprint arXiv:1511.05483*.
- Del Moral, P. (2004) *Feynman-Kac Formulae, Genealogical and Interacting Particle Systems with Applications*. New York: Springer-Verlag.
- Del Moral, P., Doucet, A. and Jasra, A. (2006) Sequential Monte Carlo samplers. *Journal of the Royal Statistical Society: Series B (Statistical Methodology)*, **68**, 411–436.
- Del Moral, P. and Murray, L. M. (2015) Sequential monte carlo with highly informative observations. *SIAM/ASA Journal on Uncertainty Quantification*, **3**, 969–997.
- Deligiannidis, G., Doucet, A. and Pitt, M. K. (2015) The correlated pseudo-marginal method. *arXiv preprint arXiv:1511.04992*.
- Diaconis, P. and Freedman, D. (1999) Iterated random functions. *SIAM review*, **41**, 45–76.
- Douc, R. and Cappé, O. (2005) Comparison of resampling schemes for particle filtering. In *Proceedings of the 4th International Symposium on Image and Signal Processing and Analysis (ISPA)*, 64–69.
- Doucet, A., de Freitas, N. and Gordon, N. (2001) *Sequential Monte Carlo methods in practice*. Springer-Verlag, New York.
- Doucet, A. and Johansen, A. (2011) A tutorial on particle filtering and smoothing: Fifteen years later. In *Handbook of Nonlinear Filtering*. Oxford, UK: Oxford University Press.

- Doucet, A., Pitt, M., Deligiannidis, G. and Kohn, R. (2015) Efficient implementation of Markov chain Monte Carlo when using an unbiased likelihood estimator. *Biometrika*, **102**, 295–313.
- Gerber, M. and Chopin, N. (2015) Sequential quasi Monte Carlo. *Journal of the Royal Statistical Society: Series B (Statistical Methodology)*, **77**, 509–579.
- Glasserman, P. and Yao, D. D. (1992) Some guidelines and guarantees for common random numbers. *Management Science*, **38**, 884–908.
- Glynn, P. W. and Rhee, C.-H. (2014) Exact estimation for Markov chain equilibrium expectations. *J. Appl. Probab.*, **51A**, 377–389.
- Glynn, P. W. and Whitt, W. (1992) The asymptotic efficiency of simulation estimators. *Operations Research*, **40**, 505–520.
- Gordon, N., Salmond, J. and Smith, A. (1993) A novel approach to non-linear/non-Gaussian Bayesian state estimation. *IEE Proceedings on Radar and Signal Processing*, **140**, 107–113.
- Guarniero, P., Johansen, A. M. and Lee, A. (2015) The iterated auxiliary particle filter. *arXiv preprint arXiv:1511.06286*.
- Jacob, P. E. (2015) Sequential Bayesian inference for implicit hidden Markov models and current limitations. *ESAIM: Proceedings and Surveys*, **51**, 24–48.
- Jacob, P. E., Murray, L. M. and Rubenthaler, S. (2015) Path storage in the particle filter. *Statistics and Computing*, **25**, 487–496.
- Jasra, A., Kamatani, K., Law, K. J. and Zhou, Y. (2015) Multilevel particle filter. *arXiv preprint arXiv:1510.04977*.
- Jones, E., Parslow, J. and Murray, L. (2010) A Bayesian approach to state and parameter estimation in a phytoplankton-zooplankton model. *Australian Meteorological and Oceanographic Journal*, **59**, 7–16.
- Jun, S.-H., Wang, L. and Bouchard-Côté, A. (2012) Entangled Monte Carlo. In *Advances in Neural Information Processing Systems (NIPS)*, 2726–2734.
- Kahn, H. and Marshall, A. W. (1953) Methods of reducing sample size in Monte Carlo computations. *Journal of the Operations Research Society of America*, **1**, 263–278.
- Kantas, N., Doucet, A., Singh, S. S., Maciejowski, J. and Chopin, N. (2015) On particle methods for parameter estimation in state-space models. *Statistical science*, **30**, 328–351.
- Lee, A. (2008) *Towards smooth particle filters for likelihood estimation with multivariate latent variables*. Master’s thesis, University of British Columbia.



- Lee, A., Doucet, A. and Łatuszyński, K. (2014) Perfect simulation using atomic regeneration with application to sequential Monte Carlo. *ArXiv e-prints*.
- Lee, A. and Holmes, C. (2010) Comment on Particle Markov chain Monte Carlo by Andrieu, Doucet and Holenstein. *Journal of the Royal Statistical Society: Series B (Statistical Methodology)*, **72**, 357–385.
- Lee, A. and Whiteley, N. (2015a) Forest resampling for distributed sequential Monte Carlo. *Statistical Analysis and Data Mining: The ASA Data Science Journal*.
- (2015b) Variance estimation and allocation in the particle filter. *arXiv preprint arXiv:1509.00394*.
- Lindsten, F., Douc, R. and Moulines, E. (2015) Uniform ergodicity of the particle Gibbs sampler. *Scandinavian Journal of Statistics*, **42**, 775–797.
- Lindsten, F., Jordan, M. I. and Schön, T. B. (2014) Particle Gibbs with ancestor sampling. *Journal of Machine Learning Research (JMLR)*, **15**, 2145–2184.
- Lindsten, F. and Schön, T. B. (2013) Backward simulation methods for Monte Carlo statistical inference. *Foundations and Trends in Machine Learning*, **6**, 1–143.
- Lindvall, T. (2002) *Lectures on the coupling method*. Courier Corporation.
- Malik, S. and Pitt, M. K. (2011) Particle filters for continuous likelihood evaluation and maximisation. *Journal of Econometrics*, **165**, 190–209.
- McLeish, D. (2012) A general method for debiasing a Monte Carlo estimator. *Monte Carlo methods and applications*, **17**, 301–315.
- Murray, L. M., Lee, A. and Jacob, P. E. (2015) Parallel resampling in the particle filter. *Journal of Computational and Graphical Statistics*.
- Naesseth, C. A., Lindsten, F. and Schön, T. B. (2014) Sequential Monte Carlo for graphical models. In *Advances in Neural Information Processing Systems (NIPS) 27*. Montreal, Quebec, Canada.
- Pitt, M. K. (2002) Smooth particle filters for likelihood evaluation and maximisation. *Technical report, University of Warwick, Department of Economics*.
- Poyiadjis, G., Doucet, A. and Singh, S. S. (2011) Particle approximations of the score and observed information matrix in state space models with application to parameter estimation. *Biometrika*, **98**, 65–80.
- Rhee, C. (2013) *Unbiased Estimation with Biased Samplers*. Ph.D. thesis, Stanford University. URL: <http://purl.stanford.edu/nf154yt1415>.

- Rhee, C. and Glynn, P. W. (2012) A new approach to unbiased estimation for SDE’s. In *Proceedings of the Winter Simulation Conference*, 17:1–17:7.
- Ruiz, H.-C. and Kappen, H. (2016) Particle smoothing for hidden diffusion processes: Adaptive path integral smoother. *arXiv preprint arXiv:1605.00278*.
- Sen, D., Thiery, A. and Jasra, A. (2016) On coupling particle filter trajectories. *arXiv preprint arXiv:1606.01016*.
- The CGAL Project (2016) *CGAL User and Reference Manual*. CGAL Editorial Board, 4.8 edn. URL: <http://doc.cgal.org/4.8/Manual/packages.html>.
- Vihola, M. (2015) Unbiased estimators and multilevel Monte Carlo. *arXiv preprint arXiv:1512.01022*.
- Whiteley, N. (2010) Comment on Particle Markov chain Monte Carlo by Andrieu, Doucet and Holenstein. *Journal of the Royal Statistical Society: Series B (Statistical Methodology)*, **72**, 357–385.
- (2013) Stability properties of some particle filters. *Ann. Appl. Probab.*, **23**, 2500–2537.
- Williams, D. (1991) *Probability with martingales*. Cambridge university press.

## A Joint or conditional sampling of particle filters

If we are interested in estimating two likelihoods  $p(y_{1:T}|\theta)$  and  $p(y_{1:T}|\tilde{\theta})$ , for known values of  $\theta$  and  $\tilde{\theta}$ , we can run a coupled particle filter in one forward pass, as described in Section 2.2. Likewise, the coupled conditional particle filter given two reference trajectories can be run in one forward pass. However, we might need to correlate  $\hat{p}^N(y_{1:T}|\theta)$  with  $\hat{p}^N(y_{1:T}|\tilde{\theta})$  for various values of  $\tilde{\theta}$  which are not known in advance, as in the setting of Metropolis–Hastings schemes in Section 3.2.

To address this situation, we can run a first particle filter given  $\theta$ , and store all the generated particles  $(\mathbf{w}_t, \mathbf{x}_t)$ , ancestors  $\mathbf{a}_t$  and random numbers  $\mathbf{U}_t$  for all  $t$ . We can later run a second particle filter, given  $\tilde{\theta}$ , conditionally on the variables generated by the first filter. At each resampling step, a probability matrix  $P_t$  is computed given the variables generated thus far. The ancestry vector  $\tilde{\mathbf{a}}_t$  is then sampled according to  $P_t$ , conditionally upon the ancestors  $\mathbf{a}_t$  from the first filter. Conditional sampling from  $P_t$  can be done in order  $N$  operations for index-coupled resampling, in order  $N \log N$  for sorted resampling and in order  $N^2$  for generic coupled resampling schemes such as transport resampling.

Storing all the generated variables incurs a memory cost of order  $N \times T$ . By carefully storing and resetting the state of the random number generator, one can in principle re-compute the first particle filter during the run of the second one, and thus the memory cost can be reduced to  $N$ ,

in exchange of a two-fold increase in computational cost and a more sophisticated implementation (see e.g. [Jun et al., 2012](#), for a similar discussion).

## B Validity of correlated particle marginal MH

We give a sufficient condition on the coupled resampling scheme for the correlated particle marginal MH algorithm to target the same distribution as the standard particle marginal MH algorithm.

Let  $r(d\mathbf{a}_t|\mathbf{w}_t)$  denote the probability distribution of the ancestors  $\mathbf{a}_t$  at step  $t$ . Since the weights  $\mathbf{w}_t$  are deterministic functions of  $\mathbf{a}_{0:t-1}$ ,  $\mathbf{U}_{0:t}$ , and  $\theta$ , we can also write  $r(d\mathbf{a}_t|\mathbf{a}_{0:t-1}, \mathbf{U}_{0:t}, \theta)$ . In the proposed algorithm,  $(\mathbf{w}_t, \mathbf{x}_t)$  and  $(\tilde{\mathbf{w}}_t, \tilde{\mathbf{x}}_t)$  are used to compute a probability matrix  $P_t$  and then  $\tilde{\mathbf{a}}_t$  are sampled conditionally on  $\mathbf{a}_t$  as described in [Appendix A](#). We denote that conditional distribution by  $c(\tilde{\mathbf{a}}_t|\mathbf{a}_{0:t-1}, \tilde{\mathbf{U}}_{0:t}, \tilde{\theta}, \mathbf{a}_{0:t}, \mathbf{U}_{0:t}, \theta)$ .

**Lemma B.1.** Assume that the marginal and conditional resampling distribution, respectively  $r$  and  $c$ , associated with the coupled resampling scheme, are such that

$$\begin{aligned} r(\mathbf{a}_t|\mathbf{a}_{0:t-1}, \mathbf{U}_{0:t}, \theta) c(\tilde{\mathbf{a}}_t|\mathbf{a}_{0:t-1}, \tilde{\mathbf{U}}_{0:t}, \tilde{\theta}, \mathbf{a}_{0:t}, \mathbf{U}_{0:t}, \theta) \\ = r(\tilde{\mathbf{a}}_t|\mathbf{a}_{0:t-1}, \tilde{\mathbf{U}}_{0:t}, \tilde{\theta}) c(\mathbf{a}_t|\mathbf{a}_{0:t-1}, \mathbf{U}_{0:t}, \theta, \tilde{\mathbf{a}}_{0:t}, \tilde{\mathbf{U}}_{0:t}, \tilde{\theta}). \end{aligned} \quad (4)$$

Furthermore, assume that under the marginal resampling distribution  $r$ ,  $\mathbb{P}(a_t^k = j) = w_t^j$  for all  $k$  and  $j$  in  $1 : N$ . Then the Markov kernel defined on  $\theta$ ,  $\mathbf{U}_{0:T}$  and  $\mathbf{a}_{0:T-1}$  by the correlated particle marginal MH algorithm has the same invariant distribution as the standard particle marginal MH.

We first provide the proof of [Lemma B.1](#), and then we show that the condition of [Eq. \(4\)](#) is satisfied for sorted, index-coupled and transport resampling schemes.

*Lemma B.1.* The extended target distribution of the particle marginal MH algorithm has density

$$\bar{\pi}(\theta, \mathbf{U}_{0:T}, \mathbf{a}_{0:T-1}) = \frac{p(\theta|y_{1:T})\varphi(\mathbf{U}_{0:T-1})\prod_{t=0}^{T-1} r(\mathbf{a}_t|\mathbf{a}_{0:t-1}, \mathbf{U}_{0:t}, \theta)\hat{p}^N(y_{1:T}|\theta)}{p(y_{1:T}|\theta)}, \quad (5)$$

which is just a change of notation compared to [Andrieu et al. \(2010\)](#). The condition  $\mathbb{P}(a_t^k = j) = w_t^j$  for all  $k$  and  $j$  in  $1 : N$  ensures that the marginal distribution on  $\theta$  is indeed the posterior distribution  $p(d\theta|y_{1:T})$ .

We denote by  $\xi$  all the auxiliary variables generated by the particle filter:  $\mathbf{U}_t$  for all  $t \in 0 : T$ , and  $\mathbf{a}_t$  for all  $t \in 0 : T - 1$ . The extended target distribution of [Eq. \(5\)](#) can be rewritten  $\bar{\pi}(\theta, \xi) = p(\theta|y_{1:T})m_\theta(\xi)\hat{p}^N(y_{1:T}|\theta)/p(y_{1:T}|\theta)$ , where  $m_\theta(\xi)$  is the distribution of  $\xi$  defined by a run of the particle filter.

Rewriting the procedure described in [Section 3.2](#), from the state  $(\theta, \xi)$ , we sample  $\tilde{\theta} \sim q(d\tilde{\theta}|\theta)$  and  $\tilde{\xi} \sim K_{\theta, \tilde{\theta}}(d\tilde{\xi}|\xi)$  from a Markov kernel on the space of  $\xi$ , which may depend on  $\theta$  and  $\tilde{\theta}$ . The

particle marginal MH algorithm uses  $K_{\theta, \tilde{\theta}}(\tilde{\xi}|\xi) = m_{\tilde{\theta}}(\tilde{\xi})$ . Other kernels leaving  $\bar{\pi}(d\theta, d\xi)$  invariant can be constructed, a sufficient condition being the standard detailed balance:

$$m_{\theta}(\xi)K_{\theta, \tilde{\theta}}(\tilde{\xi}|\xi) = m_{\tilde{\theta}}(\tilde{\xi})K_{\tilde{\theta}, \theta}(\xi|\tilde{\xi}), \quad \forall \theta, \tilde{\theta}, \xi, \tilde{\xi}. \quad (6)$$

We consider kernels  $K_{\theta, \tilde{\theta}}$  of the form

$$K_{\theta, \tilde{\theta}}(\tilde{\xi}|\xi) = \phi(\tilde{\mathbf{U}}_{0:T}|\mathbf{U}_{0:T}) \prod_{t=0}^{T-1} c(\tilde{\mathbf{a}}_t|\tilde{\mathbf{a}}_{0:t-1}, \tilde{\mathbf{U}}_{0:t}, \tilde{\theta}, \mathbf{a}_{0:t}, \mathbf{U}_{0:t}, \theta).$$

In this expression,  $\phi$  is a Markov kernel in detailed balance with respect to  $\varphi$ , the distribution of the process-generating variables. The condition of Eq. (4) implies Eq. (6). ■ □

For independent and sorted resampling, the conditional sampling of  $\tilde{\mathbf{a}}_t$  does not require any variable from the first particle system, so that we have

$$c(\tilde{\mathbf{a}}_t|\tilde{\mathbf{a}}_{0:t-1}, \tilde{\mathbf{U}}_{0:t}, \tilde{\theta}, \mathbf{a}_{0:t}, \mathbf{U}_{0:t}, \theta) = r(\tilde{\mathbf{a}}_t|\tilde{\mathbf{a}}_{0:t-1}, \tilde{\mathbf{U}}_{0:t}, \tilde{\theta}),$$

and the condition of Eq. (4) is satisfied.

For general coupled resampling schemes, under conditional sampling, for each  $k \in 1 : N$ ,  $\tilde{a}_t^k$  is distributed according to the  $a_t^k$ -th row of  $P_t$  defined by a coupled resampling scheme, e.g. Eq. (1) for index-coupled resampling. The conditional probability  $c(\tilde{\mathbf{a}}_t|\tilde{\mathbf{a}}_{0:t-1}, \tilde{\mathbf{U}}_{0:t}, \tilde{\theta}, \mathbf{a}_{0:t}, \mathbf{U}_{0:t}, \theta)$  takes the form  $\prod_{k=1}^N P_t^{a_t^k \tilde{a}_t^k} / w_t^{a_t^k}$ . For the index-coupled probability matrix of Eq. (1), Eq. (4) is satisfied, with respect to  $r(\mathbf{a}_t|\mathbf{a}_{0:t-1}, \mathbf{U}_{0:t}, \theta) = \prod_{k=1}^N w_t^{a_t^k}$ , because we obtain the transpose of  $P_t$  if we swap  $\mathbf{w}$  and  $\tilde{\mathbf{w}}$  in its construction.

For transport resampling, the distance matrix  $D$  in Section 2.3 is such that we obtain its transpose if  $\mathbf{x}$  and  $\tilde{\mathbf{x}}$  are swapped in its construction. Thus, the optimal transport probability matrix  $P_t$  is such that we obtain its transpose if  $(\mathbf{w}, \mathbf{x})$  and  $(\tilde{\mathbf{w}}, \tilde{\mathbf{x}})$  are swapped in its definition. Therefore, if  $\tilde{a}_t^k$  is distributed according to  $P_t^{a_t^k}$  for each  $k \in 1 : N$ , then the condition of Eq. (4) will be satisfied.

However, if we use an approximate solution  $\hat{P}$  to the transport problem, then the condition might not hold. This can be circumvented by symmetrizing the coupled resampling matrix, by computing  $\hat{P}$  using  $((\mathbf{w}, \mathbf{x}), (\tilde{\mathbf{w}}, \tilde{\mathbf{x}}))$ , and  $\tilde{P}$  using  $((\tilde{\mathbf{w}}, \tilde{\mathbf{x}}), (\mathbf{w}, \mathbf{x}))$ . Then one can use the matrix  $\hat{P}_t = (\hat{P} + \tilde{P}^\top)/2$ , and sample  $\tilde{a}_t^k$  distributed according to  $\hat{P}_t^{a_t^k}$  for each  $k \in 1 : N$ . This ensures that the detailed balance condition holds with respect to the multinomial resampling distribution.

## C Validity of Rhee–Glynn smoothing estimators

We first state a result on the probability of meeting in one step of the coupled conditional particle filter.

**Lemma C.1.** Under Assumptions 1 and 2, there exists  $\varepsilon > 0$  such that

$$\forall X \in \mathbb{X}^{T+1}, \quad \forall \tilde{X} \in \mathbb{X}^{T+1}, \quad \mathbb{P}(X' = \tilde{X}' | X, \tilde{X}) \geq \varepsilon,$$

where  $(X', \tilde{X}') \sim \text{CCPF}(X, \tilde{X}, U)$  and  $U \sim \varphi$ . Furthermore, if  $X = \tilde{X}$ , then  $X' = \tilde{X}'$  almost surely.

The constant  $\varepsilon$  depends on  $N$  and  $T$ , and on the coupled resampling scheme being used. Lemma C.1 can be used, together with the coupling inequality (Lindvall, 2002), to prove the ergodicity of the conditional particle filter kernel, which is akin to the approach of Chopin and Singh (2015). The coupling inequality states that the total variation distance between  $X^{(n)}$  and  $\tilde{X}^{(n-1)}$  is less than  $2\mathbb{P}(\tau > n)$ , where  $\tau$  is the meeting time. By assuming  $\tilde{X}^{(0)} \sim \pi$ ,  $\tilde{X}^{(n)}$  follows  $\pi$  at each step  $n$ , and we obtain a bound for the total variation distance between  $X^{(n)}$  and  $\pi$ . Using Lemma C.1, we can bound the probability  $\mathbb{P}(\tau > n)$  from above by  $(1 - \varepsilon)^n$ , as in the proof of Theorem 3.1 below. This implies that the computational cost of the proposed estimator has a finite expectation for all  $N \geq 2$  and  $T$ .

### C.1 Proof of Lemma C.1

Dropping the parameter from the notation, we use  $f(dx_t|x_{t-1})$  for the transition,  $m_0(dx_0)$  for the initial distribution and  $g_t(x_t) = g(y_t|x_t)$  for the measurement. Let  $\mathcal{F}_t$  denote the filtrations generated by the coupled conditional particle filter at time  $t$ . We denote by  $x_{0:t}^k$ , for  $k \in 1 : N$ , the surviving trajectories at time  $t$ .

Let  $I_t \subseteq 1 : N - 1$  be the set of common particles at time  $t$  defined by  $I_t = \{j \in 1 : N - 1 : x_{0:t}^j = \tilde{x}_{0:t}^j\}$ . The meeting probability, implicitly conditioned upon the reference trajectories  $x_{0:T}$  and  $\tilde{x}_{0:T}$ , can be bounded by:

$$\begin{aligned} \mathbb{P}(x'_{0:T} = \tilde{x}'_{0:T}) &= \mathbb{E} \left[ \mathbb{1} \left( x_{0:T}^{b_T} = \tilde{x}_{0:T}^{\tilde{b}_T} \right) \right] \geq \sum_{k=1}^{N-1} \mathbb{E}[\mathbb{1}(k \in I_T) P_T^{kk}] \\ &= (N-1) \mathbb{E}[\mathbb{1}(1 \in I_T) P_T^{11}] \geq \frac{N-1}{(N\bar{g})^2} \mathbb{E}[\mathbb{1}(1 \in I_T) g_T(x_T^1) g_T(\tilde{x}_T^1)], \end{aligned} \quad (7)$$

where we have used Assumptions 1 and 2. Now, let  $\psi_t : \mathbb{X}^t \mapsto \mathbb{R}_+$  and consider

$$\mathbb{E}[\mathbb{1}(1 \in I_t) \psi_t(x_{0:t}^1) \psi_t(\tilde{x}_{0:t}^1)] = \mathbb{E}[\mathbb{1}(1 \in I_t) \psi_t(x_{0:t}^1)^2], \quad (8)$$

since the two trajectories agree on  $\{1 \in I_t\}$ . We have

$$\mathbb{1}(1 \in I_t) \geq \sum_{k=1}^{N-1} \mathbb{1}(k \in I_{t-1}) \mathbb{1}(a_{t-1}^1 = \tilde{a}_{t-1}^1 = k), \quad (9)$$

and thus

$$\begin{aligned}
& \mathbb{E}[\mathbb{1}(1 \in I_t) \psi_t(x_{0:t}^1)^2] \\
& \geq \mathbb{E}\left[\sum_{k=1}^{N-1} \mathbb{1}(k \in I_{t-1}) \mathbb{E}[\mathbb{1}(a_{t-1}^1 = \tilde{a}_{t-1}^1 = k) \psi_t(x_{0:t}^1)^2 \mid \mathcal{F}_{t-1}]\right] \\
& = (N-1) \mathbb{E}[\mathbb{1}(1 \in I_{t-1}) \mathbb{E}[\mathbb{1}(a_{t-1}^1 = \tilde{a}_{t-1}^1 = 1) \psi_t(x_{0:t}^1)^2 \mid \mathcal{F}_{t-1}]]. \quad (10)
\end{aligned}$$

The inner conditional expectation can be computed as

$$\begin{aligned}
& \mathbb{E}[\mathbb{1}(a_{t-1}^1 = \tilde{a}_{t-1}^1 = 1) \psi_t(x_{0:t}^1)^2 \mid \mathcal{F}_{t-1}] \\
& = \sum_{k,\ell=1}^N P_{t-1}^{k\ell} \mathbb{1}(k = \ell = 1) \int \psi_t((x_{0:t-1}^k, x_t))^2 f(dx_t | x_{t-1}^k) \\
& = P_{t-1}^{11} \int \psi_t((x_{0:t-1}^1, x_t))^2 f(dx_t | x_{t-1}^1) \\
& \geq \frac{g_{t-1}(x_{t-1}^1) g_{t-1}(\tilde{x}_{t-1}^1)}{(N\bar{g})^2} \left( \int \psi_t((x_{0:t-1}^1, x_t)) f(dx_t | x_{t-1}^1) \right)^2, \quad (11)
\end{aligned}$$

where we have again used Assumptions 1 and 2. Furthermore, on  $\{1 \in I_{t-1}\}$  it holds that  $x_{0:t-1}^1 = \tilde{x}_{0:t-1}^1$  and therefore, combining Eqs. (8)–(11) we get

$$\begin{aligned}
& \mathbb{E}[\mathbb{1}(1 \in I_t) \psi_t(x_{0:t}^1) \psi_t(\tilde{x}_{0:t}^1)] \\
& \geq \frac{(N-1)}{(N\bar{g})^2} \mathbb{E}\left[\mathbb{1}(1 \in I_{t-1}) g_{t-1}(x_{t-1}^1) \int \psi_t((x_{0:t-1}^1, x_t)) f(dx_t | x_{t-1}^1) \right. \\
& \quad \left. \times g_{t-1}(\tilde{x}_{t-1}^1) \int \psi_t((\tilde{x}_{0:t-1}^1, x_t)) f(dx_t | \tilde{x}_{t-1}^1) \right]. \quad (12)
\end{aligned}$$

Thus, if we define for  $t = 1, \dots, T-1$ ,  $\psi_t(x_{0:t}) = g_t(x_t) \int \psi_{t+1}(x_{0:t+1}) f(dx_{t+1} | x_t)$ , and  $\psi_T(x_{0:T}) = g_T(x_T)$ , it follows that

$$\begin{aligned}
\mathbb{P}(x'_{0:T} = \tilde{x}'_{0:T}) & \geq \frac{(N-1)^T}{(N\bar{g})^{2T}} \mathbb{E}[\mathbb{1}(1 \in I_1) \psi_1(x_1^1) \psi_1(\tilde{x}_1^1)] \\
& = \frac{(N-1)^T}{(N\bar{g})^{2T}} \mathbb{E}[\psi_1(x_1^1)^2] \geq \frac{(N-1)^T}{(N\bar{g})^{2T}} Z^2 > 0,
\end{aligned}$$

where  $Z > 0$  is the normalizing constant of the model, defined as  $\mathbb{E}[\prod_{t=1}^T g_t(x_t)]$  where the expectation is with respect to the distribution  $m_0(dx_0) \prod_{t=1}^T f(dx_t | x_{t-1})$  of the latent process  $x_{0:T}$ .

We note that, for any fixed  $T$ , the bound goes to zero when  $N \rightarrow \infty$ . The proof fails to capture accurately the behaviour of  $\varepsilon$  in Lemma C.1 as a function of  $N$  and  $T$ .

## C.2 Proof of Theorem 3.1

We present a proof for a generalization of the estimator given in Section 3.3. Introduce a truncation variable  $G$ , with support on the integers  $\{0, 1, 2, \dots\}$ . Define the estimator as

$$H = \sum_{n=0}^G \frac{\Delta^{(n)}}{\mathbb{P}(G \geq n)}, \quad (13)$$

where  $\Delta^{(0)} = h(X^{(0)})$  and  $\Delta^{(n)} = h(X^{(n)}) - h(\tilde{X}^{(n-1)})$ , for  $n \geq 1$ . We consider the following assumption on the truncation variable.

**Assumption 4.** The truncation variable  $G$  is Geometric, with probability mass function  $\mathbb{P}(G = n) = (1 - p)^n p$ , with support on  $\{0, 1, 2, \dots\}$  and parameter  $p \in [0, 1)$ , chosen such that  $p < 1 - (1 - \varepsilon)^{\delta/(2+\delta)}$ , where  $\varepsilon$  is as in Lemma C.1 and  $\delta$  as in Assumption 3. Furthermore,  $G$  is independent of all the other variables used in Eq. (13).

This assumption precludes the use of a range of values of  $p$  near one, which could have been a tempting choice for computational reasons. On the other hand, it does not prevent the use of values of  $p$  near 0, so that we retrieve the estimator of Eq. (3) by setting  $p = 0$ , ensuring that Assumption 4 is satisfied for all values of  $\varepsilon$  and  $\delta$ .

We can first upper-bound  $\mathbb{P}(\tau > n)$ , for all  $n \geq 2$ , using Lemma C.1 (see e.g. Williams (1991), exercise E.10.5). We obtain for all  $n \geq 2$ ,

$$\mathbb{P}(\tau > n) \leq (1 - \varepsilon)^{n-1}. \quad (14)$$

This ensures that  $\mathbb{E}[\tau]$  is finite; and that  $\tau$  is almost surely finite. We then introduce the random variables

$$\forall m \geq 1 \quad Z_m = \sum_{n=0}^m \frac{\Delta^{(n)} \mathbf{1}(n \leq G)}{\mathbb{P}(n \leq G)}. \quad (15)$$

Since  $\tau$  is almost surely finite, and since  $\Delta^{(n)} = 0$  for all  $n \geq \tau$ , then  $Z_m \rightarrow Z_\tau = H$  almost surely when  $m \rightarrow \infty$ . We prove that  $(Z_m)_{m \geq 1}$  is a Cauchy sequence in  $L_2$ , i.e.  $\sup_{m' \geq m} \mathbb{E}[(Z_{m'} - Z_m)^2]$  goes to 0 as  $m \rightarrow \infty$ . We write

$$(Z_{m'} - Z_m)^2 = \sum_{n=m+1}^{m'} \frac{(\Delta^{(n)})^2 \mathbf{1}(n \leq G)}{\mathbb{P}(n \leq G)^2} + 2 \sum_{n=m+1}^{m'} \sum_{\ell=n+1}^{m'} \frac{\Delta^{(n)} \Delta^{(\ell)} \mathbf{1}(\ell \leq G)}{\mathbb{P}(n \leq G) \mathbb{P}(\ell \leq G)}$$

and thus, using the independence between  $G$  and  $(\Delta^{(n)})_{n \geq 0}$ ,

$$\mathbb{E}[(Z_{m'} - Z_m)^2] = \sum_{n=m+1}^{m'} \frac{\mathbb{E}[(\Delta^{(n)})^2]}{\mathbb{P}(n \leq G)} + 2 \sum_{n=m+1}^{m'} \sum_{\ell=n+1}^{m'} \frac{\mathbb{E}[\Delta^{(n)} \Delta^{(\ell)}]}{\mathbb{P}(n \leq G)}.$$



To control  $\mathbb{E}[(\Delta^{(n)})^2] = \mathbb{E}[(\Delta^{(n)})^2 \mathbf{1}(\tau > n)]$ , we use Hölder's inequality, with  $p = 1 + \delta/2$ , and  $q = (2 + \delta)/\delta$ , where  $\delta$  is as in Assumption 3,

$$\mathbb{E}[(\Delta^{(n)})^2] \leq \mathbb{E}[(\Delta^{(n)})^{2+\delta}]^{1/(1+\delta/2)} \left((1-\varepsilon)^{\delta/(2+\delta)}\right)^{n-1}.$$

Furthermore, using Assumption 3, there exists  $C_1 < \infty$  such that, for  $n_0 \in \mathbb{N}$  large enough,

$$\forall n \geq n_0 \quad \mathbb{E}[(\Delta^{(n)})^{2+\delta}]^{1/(1+\delta/2)} \leq C_1. \quad (16)$$

We write  $\eta = (1 - \varepsilon)^{\delta/(2+\delta)}$ , and take  $m$  such that  $m \geq n_0$ . Using Cauchy–Schwarz, we have for all  $n, \ell \geq m$ ,

$$\mathbb{E}[\Delta^{(n)} \Delta^{(\ell)}] \leq \left(\mathbb{E}[(\Delta^{(n)})^2] \mathbb{E}[(\Delta^{(\ell)})^2]\right)^{1/2} \leq C_1 \eta^{(n-1)/2} \eta^{(\ell-1)/2}.$$

We can now write

$$\begin{aligned} \mathbb{E}[(Z_{m'} - Z_m)^2] &\leq C_1 \sum_{n=m+1}^{m'} \frac{\eta^{n-1}}{\mathbb{P}(n \leq G)} + 2 \sum_{n=m+1}^{m'} \sum_{\ell=n+1}^{m'} \frac{C_1 \eta^{(n-1)/2} \eta^{(\ell-1)/2}}{\mathbb{P}(n \leq G)} \\ &\leq C_1 \sum_{n=m+1}^{m'} \frac{\eta^{n-1}}{\mathbb{P}(n \leq G)} + 2C_1 \sum_{n=m+1}^{m'} \frac{\eta^{n-1}}{\mathbb{P}(n \leq G)} \sqrt{\eta} \frac{1 - (\sqrt{\eta})^{m'}}{1 - (\sqrt{\eta})}. \end{aligned}$$

Under Assumption 4, we have  $\mathbb{P}(n \leq G) = (1 - p)^{n+1}$ . For the above series to go to zero when  $m \rightarrow \infty$  and  $m' \geq m$ , it is enough that  $\eta/(1-p) < 1$ . By definition of  $\eta$ , this holds if  $(1 - \varepsilon)^{\delta/(2+\delta)} < 1 - p$ , which is part of Assumption 4. Thus  $(Z_m)_{m \geq 1}$  is a Cauchy sequence in  $L_2$ .

By uniqueness of the limit, since  $(Z_m)_{m \geq 1}$  goes almost surely to  $H$ ,  $(Z_m)_{m \geq 1}$  goes to  $H$  in  $L_2$ . This shows that  $H$  has finite first two moments. We can retrieve the expectation of  $H$  by

$$\mathbb{E}Z_m = \sum_{n=0}^m \mathbb{E}[\Delta^{(n)}] = \mathbb{E}[h(X^{(m)})] \xrightarrow{m \rightarrow \infty} \pi(h),$$

according to Assumption 3. We can retrieve the second moment of  $H$  by

$$\begin{aligned} \mathbb{E}[Z_m^2] &= \sum_{n=0}^m \frac{\mathbb{E}[(\Delta^{(n)})^2]}{\mathbb{P}(n \leq G)} + 2 \sum_{n=0}^m \sum_{\ell=n+1}^m \frac{\mathbb{E}[\Delta^{(n)} \Delta^{(\ell)}]}{\mathbb{P}(n \leq G)} \\ &\xrightarrow{m \rightarrow \infty} \sum_{n=0}^{\infty} \frac{\mathbb{E}[(\Delta^{(n)})^2] + 2 \sum_{\ell=n+1}^{\infty} \mathbb{E}[\Delta^{(n)} \Delta^{(\ell)}]}{\mathbb{P}(n \leq G)}. \end{aligned}$$

## D Further variance reduction for the Rhee–Glynn estimator

A variance reduction can be achieved in the following way. Let  $M, m$  be two integers such that  $M > m \geq 0$ . Define

$$H_{m,M} = h(X^{(m)}) + \sum_{n=m+1}^M h(X^{(n)}) - h(\tilde{X}^{(n-1)}) \quad (17)$$

$$= h(X^{(M)}) + \sum_{n=m}^{M-1} h(X^{(n)}) - h(\tilde{X}^{(n)}), \quad (18)$$

We have  $\mathbb{E}[H_{m,M}] = \mathbb{E}[h(X^{(M)})]$  by Eq. (18) and using the fact that  $X^{(n)}$  and  $\tilde{X}^{(n)}$  have the same distribution. Furthermore,  $\mathbb{E}[h(X^{(M)})]$  goes to  $\pi(h)$  as  $M \rightarrow \infty$  under Assumption 3. We consider the estimator  $H_{m,\infty}$ , which can be computed in a finite time as follows.

We run Algorithm 1 until step  $\max(\tau, m)$ . If  $\tau \leq m+1$ , from Eq. (17),  $H_{m,\infty} = h(X^{(m)})$  almost surely, since  $X^{(n)} = \tilde{X}^{(n-1)}$  for all  $n \geq m+1$ . If  $\tau > m+1$ ,  $H_{m,\infty} = h(X^{(m)}) + \sum_{n=m+1}^{\tau-1} h(X^{(n)}) - h(\tilde{X}^{(n-1)})$ , again using Eq. (17). The estimator  $H_{m,\infty}$  is thus made of a single term with large probability if  $m$  is large enough; the computational cost is of  $\max(\tau, m)$  instead of  $\tau$  for the original estimator. The intuition is that the fewer terms there are in  $H_{m,\infty}$ , the smaller the variance.

Another question is whether we can average over various choices of  $m$ . We can compute  $\bar{H}_m = \sum_{n=0}^m \alpha_n H_{n,\infty}$  where  $\sum_{n=0}^m \alpha_n = 1$ ; this estimator is still unbiased. It follows (after some calculations) that

$$\bar{H}_m = \sum_{n=0}^m \alpha_n h(X^{(n)}) + \sum_{n=1}^{\tau-1} \beta_n (h(X^{(n)}) - h(\tilde{X}^{(n-1)})),$$

where  $\beta_n = \sum_{j=0}^{n-1 \wedge m} \alpha_j$ ; the choice of coefficients  $\alpha_{0:m}$  is left for future work.

## E Approximate transport

In this section, we briefly describe the approximation to the transport problem introduced in Cuturi (2013); Cuturi and Doucet (2014), which is explained along with various other methods in Benamou et al. (2015). The idea is to regularize the original transport program, with the modified objective function

$$\langle P, D \rangle - \varepsilon h(P),$$

where  $h(P) = -\sum_{i,j} P^{ij} \log P^{ij}$  is the entropy of  $P$ ,  $\langle P, D \rangle$  is the sum of the terms  $P^{ij} D^{ij}$ , and  $\varepsilon \in \mathbb{R}_+$ . When  $\varepsilon \rightarrow 0$ , minimizing the above objective over  $\mathcal{J}(\mathbf{w}, \tilde{\mathbf{w}})$  corresponds to the original optimal transport problem. We can write

$$\langle P, D \rangle - \varepsilon h(P) = \varepsilon \text{KL}(P \| \exp(-D/\varepsilon)),$$

where  $\text{KL}(S||Q) = \sum_{i,j} S^{ij} \log(S^{ij}/Q^{ij})$  and  $\exp(S)$  is the element-wise exponential of  $S$ . Minimizing the regularized transport objective is equivalent to finding the matrix  $P$  with minimal KL projection on  $K = \exp(-D/\varepsilon)$ , leading to the optimization problem

$$P^\varepsilon = \underset{P \in \mathcal{J}(\mathbf{w}, \tilde{\mathbf{w}})}{\operatorname{arginf}} \text{KL}(P||K). \quad (19)$$

Compared to the original transport problem, this program is computationally simpler. By noting that  $\mathcal{J}(\mathbf{w}, \tilde{\mathbf{w}}) = \mathcal{J}_{\mathbf{w}} \cap \mathcal{J}_{\tilde{\mathbf{w}}}$  where  $\mathcal{J}(\mathbf{w}) = \{P : P\mathbf{1} = \mathbf{w}\}$  and  $\mathcal{J}(\tilde{\mathbf{w}}) = \{P : P^\top \mathbf{1} = \tilde{\mathbf{w}}\}$ , we can find the solution of Eq. (19) by starting from  $P^{(0)} = K$ , and by performing iterative KL projections on  $\mathcal{J}(\mathbf{w})$  and  $\mathcal{J}(\tilde{\mathbf{w}})$ , thus constructing a sequence of matrices  $P^{(i)}$  for  $i \in \{1, \dots, n\}$ . When  $n$  goes to infinity, the matrix  $P^{(n)}$  converges to  $P^\varepsilon$ . This is Algorithm 1 in [Cuturi \(2013\)](#), which we state for completeness in Algorithm 2 below.

The algorithm is iterative, and requires matrix-vector multiplications which cost  $\mathcal{O}(N^2)$  at every iteration. The number of steps  $n$  to achieve a certain precision can be taken independently of the number of particles  $N$ , thanks to the convexity of the objective function ([Cuturi, 2013](#)). The overall cost is thus in  $\mathcal{O}(N^2)$ . Recent and future algorithms might reduce this cost, see for instance the algorithm of [Aude et al. \(2016\)](#).

---

**Algorithm 2** Cuturi’s approximation to the optimal transport problem.

---

Input:  $\mathbf{w}, \tilde{\mathbf{w}}$ , two  $N$ -vectors of normalized weights,  $x, \tilde{x}$ , two sets of locations in  $\mathbb{X}$ ; a distance  $d$  on  $\mathbb{X}$ .

Parameters:  $\varepsilon > 0$  for the regularization,  $n$  for the number of iterations.

The element-wise division between two vectors is denoted by  $/$ ,  $\mathbf{1}$  is a column vector of ones.

1. Compute the pairwise distances  $D = (D^{ij})$  where  $D^{ij} = d(x^i, \tilde{x}^j)$ .
  2. Compute  $K = \exp(-D/\varepsilon)$  (element-wise) and set  $v^{(0)} = \mathbf{1}$ .
  3. For  $i \in \{1, \dots, n\}$ ,
    - (a)  $u^{(i)} \leftarrow \mathbf{w} / (K v^{(i-1)})$ ,
    - (b)  $v^{(i)} \leftarrow \tilde{\mathbf{w}} / (K^\top u^{(i)})$ .
  4. Compute  $\hat{P}$  as  $\text{diag}(u^{(n)}) K \text{diag}(v^{(n)})$ .
- 

There are two tuning parameters: the regularization parameter  $\varepsilon$  and the number of iterations  $n$ . For  $\varepsilon$ , we follow [Cuturi \(2013\)](#) and set a small proportion of the median of the distance matrix  $D$ . For instance, we can set  $\varepsilon = 10\% \times \text{median}(D)$ . For the choice of  $n$ , we use the following adaptive criterion.

As described in Section 2.3, once the approximate solution  $\hat{P}$  is obtained by Algorithm 2, we need to correct its marginals. We compute the approximate marginals  $\mathbf{u} = \hat{P}\mathbf{1}$  and  $\tilde{\mathbf{u}} = \hat{P}^\top\mathbf{1}$ , and set

$$\alpha = \min_{i \in 1:N} \left( \min \left( \frac{w_i}{u_i}, \frac{\tilde{w}_i}{\tilde{u}_i} \right) \right), \quad \mathbf{r} = \frac{\mathbf{w} - \alpha \mathbf{u}}{1 - \alpha}, \quad \tilde{\mathbf{r}} = \frac{\tilde{\mathbf{w}} - \alpha \tilde{\mathbf{u}}}{1 - \alpha}.$$

The final transport probability matrix is given by  $P = \alpha \hat{P} + (1 - \alpha) \mathbf{r} \tilde{\mathbf{r}}^\top$ . When  $n$  increases,  $\hat{P} = P^{(n)}$  gets nearer to the regularized solution  $P^\varepsilon$  which is in  $\mathcal{J}(\mathbf{w}, \tilde{\mathbf{w}})$ . Accordingly, when  $n$  increases we can take  $\alpha$  close to one. This gives a heuristic approach to choose  $n$ : we stop Algorithm 2 when the current solution  $P^{(n)} = \text{diag}(u^{(n)}) K \text{diag}(v^{(n)})$  is such that  $\alpha$  computed above is at least a certain value, for instance 90%. This ensures that the transport probability matrix  $\hat{P}$  is a close approximation to the regularized transport problem.

## F Experiments with the Rhee–Glynn smoother

We explore the sensitivity of the proposed smoother to various inputs, section by section. The experiments are based on the hidden auto-regressive model, with  $d_x = 1$ , and the data are generated with  $\theta = 0.95$ ; except in Section F.6 where we use a nonlinear model. Each experiment is replicated  $R = 1,000$  times. We do not use any variance reduction technique in this section.

### F.1 Effect of the resampling scheme

First we investigate the role of the resampling scheme. A naive scheme is systematic resampling performed on each system with a common uniform variable. A second scheme is index-coupled resampling as described in Section 2.4. In both cases, at the final step of the coupled conditional particle filter, we sample two trajectory indices  $(b_T, \tilde{b}_T)$  using systematic resampling with a common uniform variable.

We consider a time series of length  $T = 20$ . In Table 1, we give the average meeting time as a function of  $N$ , for both resampling schemes, with the standard deviation between parenthesis. First we see that the meeting time is orders of magnitude smaller when using index-coupled resampling. Secondly, we see that the meeting time tends to decrease with  $N$ , when using index-coupled resampling, whereas it increases when using systematic resampling. For longer time series, we find that the index-coupled resampling is the only viable option, and thus focus on this scheme for the Rhee–Glynn smoother.

### F.2 Effect of the number of particles

We consider the effect of the number of particles  $N$ , on the meeting time and on the variance of the resulting estimator. We use a time series of length  $T = 500$ , generated from the model. As seen in the previous section, when using index-coupled resampling, we expect the meeting time  $\tau$  to occur

	systematic	index-coupled
N = 50	482.87 (472.96)	7.95 (7.41)
N = 100	462.88 (448.37)	4.88 (3.45)
N = 150	531.69 (546.32)	4.19 (2.68)
N = 200	569.49 (575.09)	4.01 (2.34)

Table 1: Average meeting time as a function of the number of particles  $N$  and of the resampling scheme. Standard deviations are between brackets. Results obtained in the hidden auto-regressive model with  $T = 20$ .

sooner if  $N$  is larger. On the other hand, the cost of the coupled conditional particle filter is linear in  $N$ , so that the overall cost of obtaining each estimator  $H$  has expectation of order  $\mathbb{E}[\tau] \times N$ . We give estimators of this cost as a function of  $N$  in Table 2, as well as the average meeting time. We see that the cost per estimator decreases when  $N$  increases, and then increases again. There seems to be an optimal value of  $N$  yielding the minimum cost.

	cost	meeting time
N = 256	220567 (241823)	861.59 (944.62)
N = 512	17074 (17406)	33.35 (34)
N = 1024	7458 (5251)	7.28 (5.13)
N = 2048	8739 (4888)	4.27 (2.39)
N = 4096	14348 (6631)	3.5 (1.62)

Table 2: Average cost and meeting time, as a function of the number of particles  $N$ . Standard deviations are between brackets. Results obtained in the hidden auto-regressive model with  $T = 500$ .

We now consider the estimators  $H_t$  of each smoothing mean  $\mathbb{E}[x_t|y_{1:T}]$ , for  $t \in 0 : T$ , i.e. we take  $h$  to be the identity function. We compute the empirical variance of  $H_t$ , for each  $t$ , over the  $R$  experiments. To take into account both variance and computational cost, we define the efficiency as  $1/(\mathbb{V}[H_t] \times \mathbb{E}[\tau] \times N)$  and approximate this value for each  $t$ , using the  $R$  estimators. The results are shown in Figure 7.

We see that the variance explodes exponentially when  $T - t$  increases (for fixed  $T$  and increasing  $t$ ; see Section F.5 for the behaviour with  $T$ ). From Figure 7a, the variance is reduced when larger values of  $N$  are used. Secondly, the variance is most reduced for the estimators of the first smoothing means, i.e.  $\mathbb{E}[x_t|y_{1:T}]$  for small  $t$ . As such, the efficiency is maximized for the largest values of  $N$  only when  $t$  is small, as can be seen from Figure 7b. For values of  $t$  closer to  $T$ , the efficiency is higher for  $N = 1,024$  and  $N = 2,048$  than it is for  $N = 4,096$ .

### F.3 Effect of the truncation variable

We now consider the use of Geometric truncation variables, as introduced in the Appendix C. We set  $T = 500$  and  $N = 512$ . We try a few values of the Geometric probability  $p$ , in an attempt to

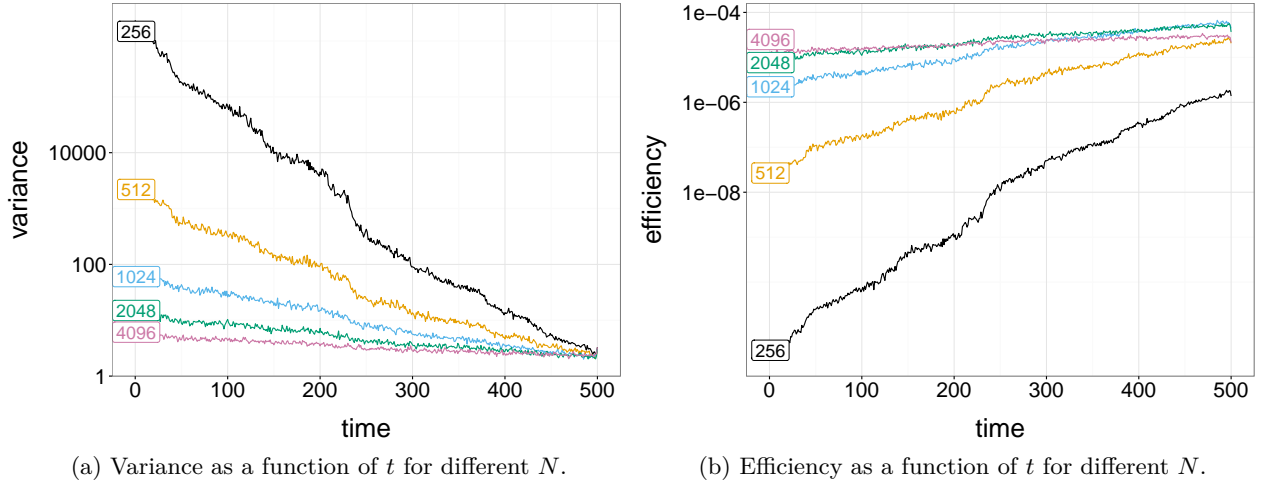


Figure 7: Variance (left) and efficiency (right) of the estimator of the smoothing mean  $\mathbb{E}[x_t|y_{1:T}]$  for  $T = 500$ , in the hidden auto-regressive model. The efficiency takes into account the computational cost of the estimator. The y-axis is on the logarithmic scale.

reduce the computation cost per estimator. The value  $p = 0$  corresponds to the estimator proposed in Section 3.3. The average meeting times are shown in Table 3.

	meeting time
$p = 0$	31.94 (31.26)
$p = 0.025$	17.66 (17.35)
$p = 0.05$	11.82 (11.68)

Table 3: Average meeting time, as a function of the Geometric parameter  $p$ . Standard deviations are between brackets. Results obtained in the hidden auto-regressive model with  $T = 500$ .

We plot the variance of the estimator of the smoothing mean  $\mathbb{E}[x_t|y_{1:T}]$  against  $t$  on Figure 8a, for each  $p$ . We plot the efficiency  $\mathbb{E}[\min(G, \tau)] \times \mathbb{V}[H_t]$  against  $t$  on Figure 8b, for each  $p$ . First, from Figure 8a, we see that increasing  $p$  leads to a higher variance. In particular, the value  $p = 0.05$  leads to a much larger variance than the other values. This seems to be in agreement with Assumption 4, which states that  $p$  has to be below a certain threshold related to the meeting probability.

On Figure 8b, we see that the increase of variance is compensated by a reduction of the computation cost, for the smaller values of  $p$ . Therefore, the three smaller values lead to the same overall efficiency. On the other hand, the largest value  $p = 0.05$  leads to a significantly lower efficiency. Thus, there does not seem to be much benefit in using  $p \neq 0$  in this example.

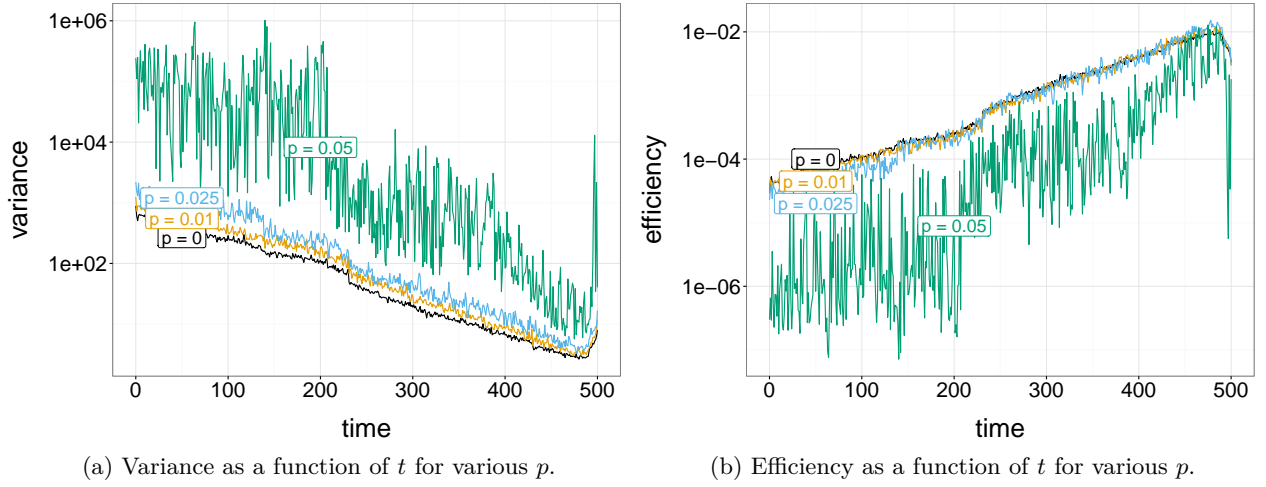


Figure 8: Variance (left) and efficiency (right) of the smoothing estimator using a Geometric truncation variable with parameter  $p$ , for  $T = 500$ , and  $N = 512$ , in the hidden auto-regressive model. The efficiency takes into account the computational cost of the estimator. The y-axis is on the logarithmic scale.

#### F.4 Effect of ancestor sampling

We consider the use of ancestor sampling, which requires being able to evaluate the transition density,  $f(x_t|x_{t-1}, \theta)$ , for all  $x_{t-1}, x_t$  and all  $\theta$ . We set  $T = 500$  as before, and consider different values of  $N$ . The average meeting times are displayed in Table 4. We see that the meeting times are significantly reduced by using ancestor sampling, especially for smaller numbers of particles.

	without ancestor sampling	with ancestor sampling
$N = 256$	861.59 (944.62)	8.79 (3.33)
$N = 512$	33.35 (34)	5.99 (2.27)
$N = 1024$	7.28 (5.13)	4.51 (1.88)
$N = 2048$	4.27 (2.39)	3.76 (1.63)
$N = 4096$	3.5 (1.62)	3.34 (1.51)

Table 4: Average meeting time, as a function of the number of particles  $N$ , with and without ancestor sampling. Standard deviations are between brackets. Results obtained in the hidden auto-regressive model with  $T = 500$ .

We consider variance and efficiency, here defined as  $1/(\mathbb{V}[H_t] \times \mathbb{E}[\tau] \times N)$ . The results are shown in Figure 9. This is to be compared with Figure 7 obtained without ancestor sampling.

First we see that the variance is significantly reduced by ancestor sampling. The variance seems to increase only slowly as  $T - t$  increases, for each value of  $N$ . From Figure 9b, we see that the smallest value of  $N$  now leads to the most efficient algorithm. In other words, for a fixed computational budget, it is more efficient to produce more estimators with  $N = 256$  than to



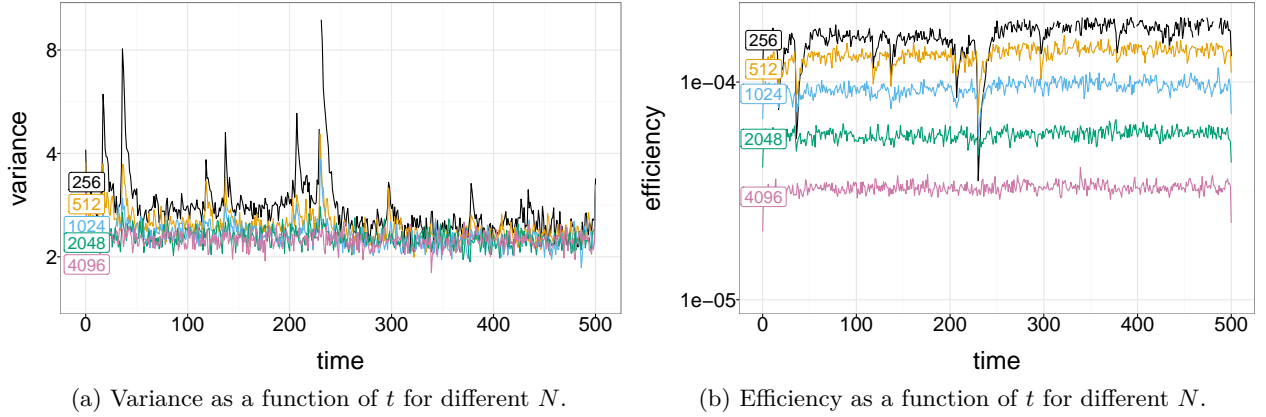


Figure 9: Variance (left) and efficiency (right) of the estimator of the smoothing mean  $\mathbb{E}[x_t|y_{1:T}]$  for  $T = 500$ , in the hidden auto-regressive model, when using ancestor sampling. The efficiency takes into account the computational cost of the estimator. The y-axis is on the logarithmic scale.

increase the number of particles and to average over fewer estimators.

### F.5 Effect of the time horizon

We investigate the effect of the time horizon  $T$ , that is, the total length of the time series, on the performance of the smoother. We expect the conditional particle filter kernel to perform less and less well when  $T$  increases. To compensate for this loss of efficiency, we increase the number of particles  $N$  linearly with  $N$ : for  $T = 64$  we use  $N = 128$ , for  $T = 128$  we use  $N = 256$ , and so forth up to  $T = 1,024$  and  $N = 2,048$ . With that scaling, the computational cost of each run of coupled conditional particle filter is quadratic in  $T$ . A first question is whether the meeting time is then stable with  $T$ . Table 5 reports the average meeting times obtained when scaling  $N$  linearly with  $T$ . We see that the meeting times occur in roughly the same number of steps, implying that the linear scaling of  $N$  with  $T$  is enough.

	without ancestor sampling	with ancestor sampling
$N = 128, T = 64$	11.73 (10.87)	6.54 (3.91)
$N = 256, T = 128$	9.51 (7.61)	5.77 (2.8)
$N = 512, T = 256$	11.25 (9.33)	5.66 (2.67)
$N = 1024, T = 512$	7.8 (6.05)	4.51 (1.81)
$N = 2048, T = 1024$	9.07 (6.82)	4.58 (1.9)

Table 5: Average meeting time, as a function of the number of particles  $N$  and the time horizon  $T$ , with and without ancestor sampling. Standard deviations are between brackets. Results obtained in the hidden auto-regressive model.

A second question is whether scaling  $N$  linearly with  $T$  is enough to ensure that the variance

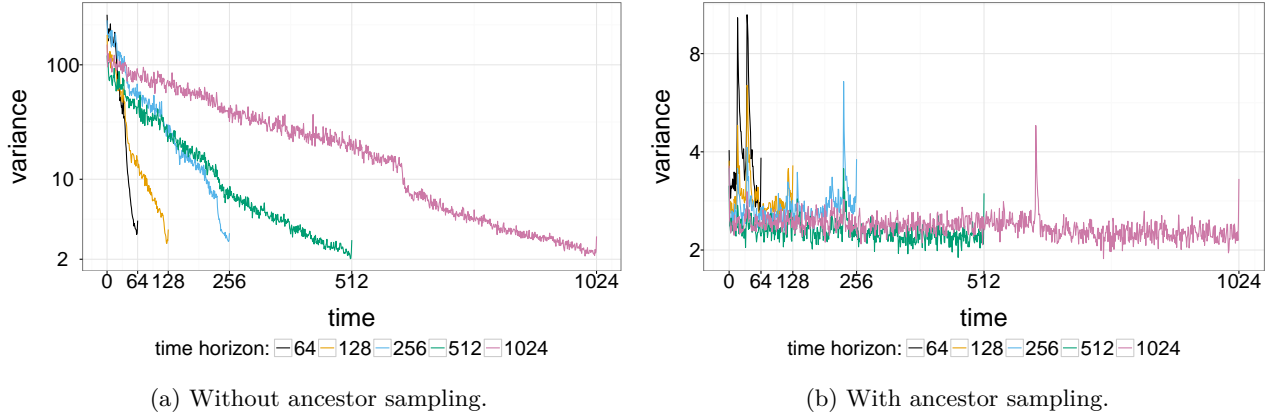


Figure 10: Variance of the estimator of the smoothing mean  $\mathbb{E}[x_t|y_{1:T}]$  for various time horizons, without (left) and with (right) ancestor sampling, in the hidden auto-regressive model. The y-axis is on the logarithmic scale.

of the resulting estimator is stable. Results are shown in Figure 10, obtained without (Figure 10a) and with ancestor sampling (Figure 10b). The plots show the variance of the estimator of the smoothing means  $\mathbb{E}[x_t|y_{1:T}]$  for all  $t \leq T$  and various  $T$ . We see that, for the values of  $t$  that are less than all the time horizons, the variance of the estimators of  $\mathbb{E}[x_t|y_{1:T}]$  seems stable with  $T$ . The experiments thus indicate that, to estimate  $\mathbb{E}[x_t|y_{1:T}]$  for all  $t$ , one can scale  $N$  linearly in  $T$  and expect the meeting time and the variance of the Rhee–Glynn estimators to be stable. Overall, the computational cost is then quadratic in  $T$ .

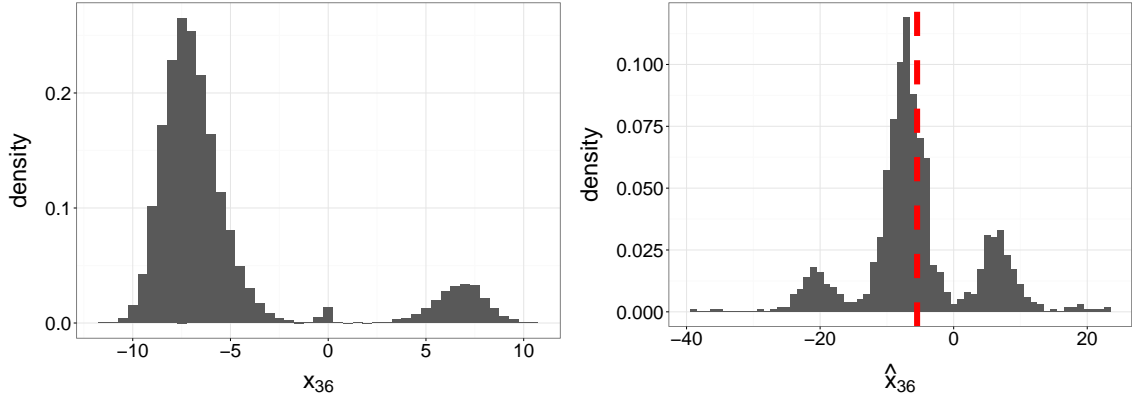
## F.6 Effect of multimodality in the smoothing distribution

We switch to another model to investigate the behaviour of the Rhee–Glynn estimator when the smoothing distribution is multimodal. We consider the nonlinear growth model used by [Gordon et al. \(1993\)](#). We set  $x_0 \sim \mathcal{N}(0, 2)$ , and, for  $t \geq 1$ ,

$$x_t = 0.5x_{t-1} + 25x_{t-1}/(1 + x_{t-1}^2) + 8\cos(1.2(t-1)) + W_t, \quad \text{and} \quad y_t = x_{t-1}^2/20 + V_t,$$

where  $W_t$  and  $V_t$  are independent normal variables, with variances 1 and 10 respectively. We generate  $T = 50$  observations using  $x_0 = 0.1$ , following [Gordon et al. \(1993\)](#). Because the measurement distribution  $g(y_t|x_t, \theta)$  depends on  $x_t$  through  $x_t^2$ , the sign of  $x_t$  is hard to identify, and as a result the smoothing distribution has multiple modes. We run a conditional particle filter with ancestor sampling, with  $N = 1,024$  particles for  $M = 50,000$  iterations, and discard the first 25,000 iterations. We plot the histogram of the obtained sample for  $p(dx_t|y_{1:T}, \theta)$  at time  $t = 36$  in Figure 11a. We notice at least two modes, located around  $-7$  and  $+7$ , with possibly an extra mode near zero.

We run the Rhee–Glynn smoother with  $N = 1,024$  and ancestor sampling. Each estimator took



(a) Approximation of the smoothing distribution, using a conditional particle filter, at  $t = 36$ . (b) Rhee–Glynn estimators of the smoothing mean, and true mean in vertical dashed (red) line, at  $t = 36$ .

Figure 11: Smoothing distribution approximated by conditional particle filters (left), and  $R = 1,000$  independent Rhee–Glynn estimators of the smoothing mean (right), at time  $t = 36$  for the nonlinear growth model with  $T = 50$ .

less than 10 iterations of the coupled conditional particle filter to meet, with a median meeting time of 3 iterations. The total number of calls to the coupled conditional particle filter to obtain  $R = 1,000$  estimators adds up to 2,984. We plot the histogram of the estimators  $H_t^{(r)}$ , for  $r \in 1 : R$ , of the smoothing mean  $\mathbb{E}[x_t|y_{1:T}]$  at time  $t = 36$  in Figure 11b. We see that the distribution of the estimator is itself multimodal. Indeed, the two initial reference trajectories might belong to the mode around  $-7$ , or to the mode around  $+7$ , or each trajectory might belong to a different mode. Each of these cases leads to a mode in the distribution of the Rhee–Glynn estimator.

The resulting estimator  $\hat{x}_t$  of each smoothing mean is obtained by averaging the  $R = 1,000$  independent estimators  $H_t^{(r)}$ . We compute the Monte Carlo standard deviation  $\hat{\sigma}_t$  at each time  $t$ , and represent the confidence intervals  $[\hat{x}_t - 2\hat{\sigma}_t/\sqrt{R}, \hat{x}_t + 2\hat{\sigma}_t/\sqrt{R}]$  as error bars in Figure 12. The line represents the smoothing means obtained by conditional particle filter with ancestor sampling, taken as ground truth. The agreement shows that the proposed method is robust to multimodality in the smoothing distribution.

## G Pseudo-code for particle filters

We provide pseudo-code for the bootstrap particle filter (Algorithm 3), the conditional particle filter (Algorithm 4), the coupled bootstrap particle filter (Algorithm 5), and the coupled conditional particle filter (Algorithm 6).

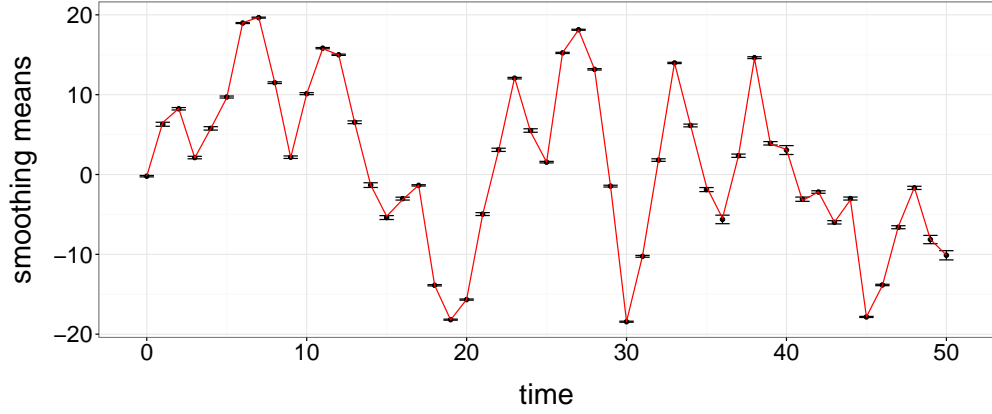


Figure 12: Confidence intervals around the exact smoothing means. The intervals are computed as two standard deviations around the mean of  $R = 1,000$  proposed smoothing estimators. The line represents the exact smoothing means, retrieved by a long run of conditional particle filter, for the nonlinear growth model with  $T = 50$  observations.

---

**Algorithm 3** Bootstrap particle filter, given a parameter  $\theta$ .

---

At step  $t = 0$ .

1. Draw  $x_0^k \sim m_0(dx_0|\theta)$ , for all  $k \in 1 : N$ .  
This can also be written  $x_0^k = M(U_0^k, \theta)$ , for all  $k \in 1 : N$ .
2. Set  $w_0^k = N^{-1}$ , for all  $k \in 1 : N$ .

At step  $t \geq 1$ .

1. Draw ancestors  $a_{t-1}^{1:N} \sim r(da^{1:N}|w_{t-1}^{1:N})$ .
2. Draw  $x_t^k \sim f(dx_t|x_{t-1}^{a_{t-1}^k}, \theta)$ , for all  $k \in 1 : N$ .  
This can also be written  $x_t^k = F(x_{t-1}^{a_{t-1}^k}, U_t^k, \theta)$ , for all  $k \in 1 : N$ .
3. Compute  $w_t^k \propto g(y_t|x_t^k, \theta)$ , for all  $k \in 1 : N$ , and normalize the weights.

Return the likelihood estimator  $\hat{p}^N(y_{1:T}|\theta) = \prod_{t=1}^T N^{-1} \sum_{k=1}^N g(y_t|x_t^k, \theta)$ .

---

---

**Algorithm 4** Conditional particle filter, given a reference trajectory  $x_{0:T}$  and  $\theta$ .

---

At step  $t = 0$ .

1. Draw  $x_0^k \sim m_0(dx_0|\theta)$ , for  $k \in 1 : N - 1$ , and set  $x_0^N = x_0$ .  
This can also be written  $x_0^k = M(U_0^k, \theta)$ , for all  $k \in 1 : N - 1$ , and  $x_0^N = x_0$ .
2. Set  $w_0^k = N^{-1}$ , for  $k \in 1 : N$ .

At step  $t \geq 1$ .

1. Draw ancestors  $a_{t-1}^{1:N-1} \sim r(da^{1:N-1}|w_{t-1}^{1:N})$ , and set  $a_{t-1}^N = N$ .
2. Draw  $x_t^k \sim f(dx_t|x_{t-1}^{a_{t-1}^k}, \theta)$ , for all  $k \in 1 : N - 1$ , and set  $x_t^N = x_t$ .  
This can also be written  $x_t^k = F(x_{t-1}^{a_{t-1}^k}, U_t^k, \theta)$ , for all  $k \in 1 : N - 1$ , and  $x_t^N = x_t$ .
3. Compute  $w_t^k \propto g(y_t|x_t^k, \theta)$ , for all  $k \in 1 : N$ , and normalize the weights.

Draw a trajectory.

1. Draw  $b_T$  from a discrete distribution on  $1 : N$ , with probabilities  $w_T^{1:N}$ .
2. For  $t = T - 1, \dots, 0$ , set  $b_t = a_t^{b_{t+1}}$ .

Return  $x'_{0:T} = (x_0^{b_0}, \dots, x_T^{b_T})$ .

---

---

**Algorithm 5** Coupled bootstrap particle filter, given parameters  $\theta$  and  $\tilde{\theta}$ .

---

At step  $t = 0$ .

1. Draw  $U_0^k$ , and compute  $x_0^k = M(U_0^k, \theta)$  and  $\tilde{x}_0^k = M(U_0^k, \tilde{\theta})$ , for all  $k \in 1 : N$ .
2. Set  $w_0^k = N^{-1}$  and  $\tilde{w}_0^k = N^{-1}$ , for all  $k \in 1 : N$ .

At step  $t \geq 1$ .

1. Compute a probability matrix  $P_{t-1}$ , with marginals  $w_{t-1}^{1:N}$  and  $\tilde{w}_{t-1}^{1:N}$ . Sample  $(a_{t-1}^k, \tilde{a}_{t-1}^k)$  from  $P_{t-1}$ , for all  $k \in 1 : N$ .
2. Draw  $U_t^k$ , and compute  $x_t^k = F(x_{t-1}^{a_{t-1}^k}, U_t^k, \theta)$  and  $\tilde{x}_t^k = F(\tilde{x}_{t-1}^{\tilde{a}_{t-1}^k}, U_t^k, \tilde{\theta})$ , for all  $k \in 1 : N$ .
3. Compute  $w_t^k \propto g(y_t | x_t^k, \theta)$  and  $\tilde{w}_t^k \propto g(y_t | \tilde{x}_t^k, \tilde{\theta})$ , for all  $k \in 1 : N$ , and normalize the weights.

Return  $\hat{p}^N(y_{1:T} | \theta) = \prod_{t=1}^T N^{-1} \sum_{k=1}^N g(y_t | x_t^k, \theta)$  and  $\hat{p}^N(y_{1:T} | \tilde{\theta}) = \prod_{t=1}^T N^{-1} \sum_{k=1}^N g(y_t | \tilde{x}_t^k, \tilde{\theta})$ .

---



---

**Algorithm 6** Coupled conditional particle filter, given reference trajectories  $x_{0:T}$  and  $\tilde{x}_{0:T}$ .

---

At step  $t = 0$ .

1. Draw  $U_0^k$ , compute  $x_0^k = M(U_0^k, \theta)$  and  $\tilde{x}_0^k = M(U_0^k, \theta)$  for  $k \in 1 : N - 1$ .
2. Set  $x_0^N = x_0$  and  $\tilde{x}_0^N = \tilde{x}_0$ .
3. Set  $w_0^k = N^{-1}$  and  $\tilde{w}_0^k = N^{-1}$ , for  $k \in 1 : N$ .

At step  $t \geq 1$ .

1. Compute a probability matrix  $P_{t-1}$ , with marginals  $w_{t-1}^{1:N}$  and  $\tilde{w}_{t-1}^{1:N}$ . Sample  $(a_{t-1}^k, \tilde{a}_{t-1}^k)$  from  $P_{t-1}$ , for all  $k \in 1 : N - 1$ . Set  $a_{t-1}^N = N$  and  $\tilde{a}_{t-1}^N = N$ .
2. Draw  $U_t^k$ , and compute  $x_t^k = F(x_{t-1}^{a_{t-1}^k}, U_t^k, \theta)$  and  $\tilde{x}_t^k = F(\tilde{x}_{t-1}^{\tilde{a}_{t-1}^k}, U_t^k, \theta)$ , for all  $k \in 1 : N - 1$ . Set  $x_t^N = x_t$  and  $\tilde{x}_t^N = \tilde{x}_t$ .
3. Compute  $w_t^k \propto g(y_t | x_t^k, \theta)$  and  $\tilde{w}_t^k \propto g(y_t | \tilde{x}_t^k, \tilde{\theta})$ , for all  $k \in 1 : N$ , and normalize the weights.

Draw a pair of trajectories.

1. Compute a probability matrix  $P_T$ , with marginals  $w_T^{1:N}$  and  $\tilde{w}_T^{1:N}$ . Draw  $(b_T, \tilde{b}_T)$  from  $P_T$ .
2. For  $t = T - 1, \dots, 0$ , set  $b_t = a_t^{b_{t+1}}$  and  $\tilde{b}_t = \tilde{a}_t^{\tilde{b}_{t+1}}$ .

Return  $x'_{0:T} = (x_0^{b_0}, \dots, x_T^{b_T})$  and  $\tilde{x}'_{0:T} = (\tilde{x}_0^{\tilde{b}_0}, \dots, \tilde{x}_T^{\tilde{b}_T})$ .

---